

EXPERIMENTAL INVESTIGATION OF M-SHAPE HEAT TRANSFER COEFFICIENT DISTRIBUTION OF R123 FLOW BOILING IN SMALL DIAMETER TUBES

Dariusz Mikielewicz, Michał Klugmann, Jan Wajs

Gdansk University of Technology, Faculty of Mechanical Engineering, Heat Technology
Department, ul. Narutowicza 11/12, 80-233 Gdansk, Poland

Email: Dariusz.Mikielewicz@pg.gda.pl, tel. +48 58 347 2254, fax. +48 58 347 2816

ABSTRACT

This paper presents a study into flow boiling of R123 in two small diameter silver tubes of inner diameters of 1.15mm and 2.3mm. The experiments have been accomplished for a wide range of quality variation (0.01 – 0.9), mass flow rate (650 -3000 kg/m²s) and heat fluxes (40 – 80 kW/m²). The saturation temperature ranged from 30 to 70°C. In experiments a peculiar distribution of heat transfer coefficient leading to development of two maxima in its distribution with respect to quality has been observed. Such behaviour was seen in both sizes of tubes.

INTRODUCTION

Boiling heat transfer, as one of the most efficient techniques for removing high heat fluxes, has been extensively studied for a very long time. Nowadays, rapid development of practical engineering applications for micro-devices, micro-systems, advanced material designs, manufacturing of compact heat exchangers, electronic microchips increases the demand for better understanding of small and micro-scale transport phenomena. There is a significant

body of experimental research into the flow boiling in small diameter channels and minichannels, however the conclusions from these studies are still not unanimous, which gives incentives for additional research.

Lazarek and Black [1], measured the local and average heat transfer coefficient, pressure drop, and critical heat flux of saturated boiling of R-113 flowing vertically upwards and downwards in single 3.17 mm tubes, $L = 123$ and 246 mm, $G = 125\text{--}750$ kg/(m²s), $p = 1.3\text{--}4.1$ bar, $q = 14\text{--}380$ kW/m², and $\Delta T_{\text{sub,in}} = 3\text{--}73$ K. The major conclusion from the study was that the heat transfer coefficient was found to be independent of the flow quality for $x \geq 0$. They concluded that nucleate boiling was the dominant heat transfer mechanism in all tests. That was based on the observed strong dependence of heat transfer coefficient on heat flux and negligible influence of quality. They suggested that the occurrence of nucleate boiling dominated heat transfer all the way to critical heat flux could be attributed to the high boiling number ($Bo > 5 \times 10^4$) of their data. Predictions from the Chen [2] and Shah [3] correlations were compared with their experimental data, concluding that the Shah correlation showed reasonable agreement with their experiments. The authors provided also their own experimental correlation to fit their data.

Wambsganss et al. [4], investigated the nucleate flow boiling of R-113 through a single tube of 2.92 mm inside diameter. Investigated range of parameters was $G = 50\text{--}300$ kg/(m²s), $p = 1.24\text{--}1.6$ bar, $q = 8.8\text{--}90.7$ kW/m², $x = 0\text{--}0.9$ and $T_{\text{in}} = 20\text{--}50$ °C. The heat transfer coefficient slightly decreased with increasing quality for $x \geq 0$. The correlation due to Lazarek and Black [1] showed the best agreement in correlating that data.

Tran et al. [5,6], measured the local heat transfer coefficients and overall two-phase pressure drop for three different refrigerants (R-113, R-12, R-134a) through both a single circular tube of 2.46 mm inner diameter and rectangular cross-sectioned channels of hydraulic diameter of

2.4 and 2.9 mm, with $G = 44\text{--}832 \text{ kg}/(\text{m}^2\text{s})$, $p = 5.1$ and 8.2 bar, $q = 3.6\text{--}129 \text{ kW}/\text{m}^2$ and $x = 0\text{--}0.94$. Their results showed different behavior of the flow boiling in small channels from that found in large hydraulic diameters. Nucleate boiling was dominant for wall superheats larger than 2.75 K , forced convective boiling for walls superheated less than 2.75K , and the heat transfer coefficient was independent of x for $x \geq 0.2$. An empirical correlation was proposed, where the heat transfer coefficient was correlated with the boiling number, Weber number, and liquid to vapor density ratio. No significant geometry effect was found between circular and rectangular channels.

Kew and Cornwell [7] found that simple nucleate boiling correlations predicted relatively well their results in single narrow tubes in the confined bubbles flow region. They also underlined the fact that pool boiling correlations often have no geometric components although the influence of surface angle and tube diameter for example have shown to be important. Nucleate boiling is enhanced in small channels at low wall superheats above that predicted by the pool boiling correlation.

Kew and Cornwell [7] investigated nucleate boiling, confined bubble boiling, partial dry-out, and convective boiling of R-141b in single tubes with $1.39\text{--}3.69$ mm inside diameter. For the larger tubes (2.87 and 3.69 mm), the heat transfer coefficient decreased slightly or remained constant with increasing x for $x \leq 0.2$, but increased for $x \geq 0.2$. For the smaller tube (1.39 mm inside diameter), the heat transfer increased with increasing x at low mass flux, G , for $x \geq 0$, but decreased rapidly at high G for $x \geq 0$.

In Bao et al. [8], the heat transfer coefficients of R-12, and R-123 flow boiling were measured for flow through a single horizontal tube of 1.95 mm inner diameter. The flow conditions were $G = 50\text{--}1800 \text{ kg}/(\text{m}^2 \text{ s})$, $p = 2\text{--}5$ bar, $q = 5\text{--}200 \text{ kW}/\text{m}^2$ and $x = 0\text{--}0.9$. The heat transfer coefficient was independent of quality for $x \geq 0$, and their data showed a strong dependence of



the heat transfer coefficient on the heat flux and the system saturation pressure, while it was independent of the mass flux and vapor quality.

Karayiannis [9] accomplished research into small diameter tubes with R-134a as test fluid. These investigations were carried out on stainless steel tubes with internal diameters of 2 mm and 4.26 mm. 996 data points were at the disposal for comparisons. The test section was 40 cm long. The flow parameters were following: $x=0.1-0.8$, $G=100-500 \text{ kg/m}^2\text{s}$, heat flux, $q=11-100 \text{ kW/m}^2$, $T_{\text{SAT}}=30-46 \text{ }^\circ\text{C}$. Both increasing and decreasing trends of heat transfer coefficient with quality were detected.

Recently, Bar-Cohen and Rahim [10] reported the existence of an M-shaped distribution of heat transfer coefficient with respect to quality in small diameter tubes. In their opinion the phenomenon is specific only to such small passages and its explanation is lacking proper validations, therefore more studies focused on that effects are required especially of the runs encompassing the whole range of quality variation.

The objective of the present study is to shed more light into the problem of flow boiling in small diameter tubes, as during experiments it turned out that the obtained distributions of heat transfer distribution with respect to quality were following in some cases the M-shaped distribution of heat transfer coefficient.

EXPERIMENTAL FACILITY

An experimental rig has been designed and constructed as a compact, highly integrated mobile unit, Fig. 1. It's main part is a closed loop of a working fluid. Freon R-123 (Suva) has been selected as a test fluid due to its very convenient saturation temperature: $27.9 \text{ }^\circ\text{C}$ under normal conditions. The flow of working fluid is forced by a set of two electrically-powered



pumps, composed in series, capable to deliver mass flow rate up to 200 kg/h and gauge pressure up to 8 bars. Gear pumps have been chosen to limit any arising flow pulsations. Adjustment of the mass flow is realized by changing voltage of the pump's power supply or using the by-pass. Working medium is pumped from the main tank through the Danfoss mass flowmeter type MASS D1 3 working with MASS 6000 19" IP20 interface. Such system, gives about 0.3 % of measurement accuracy. In the present work the mass flow range from 10 to 45 kg/h has been considered. Then the working fluid went to the pre-heater, where it attained required input parameters. Isobaric pre-heating was realized in the stainless steel tube powered by the low voltage, high current DC power supply. Such arrangement provides the power up to 1.2 kW, corresponding to heat flux of 168 kW/m^2 . In such way, the full range of quality x was possible to be obtained at the test section input. Current, voltage, inlet and outlet temperatures and pressure were measured on the pre-heater to determine a corresponding heat flux and quality x from the appropriate heat balance. From the pre-heater the medium went to the test section through the connection sockets. In this experiment a silver tube of 1.15 mm or 2.3 mm inner diameter, and the length of 38 cm was used. The working medium flowed into the test section with a pre-defined quality x and was heated further to get the expected boiling conditions. Heating in the test section was realized using a low voltage, high current DC power supply and could be adjusted from 0 up to 1 kW of heating power, corresponding to the heat flux up to 364 kW/m^2 . Current, voltage, inlet temperature, inlet pressure, outlet temperature and outlet pressure were measured at the test section to determine the corresponding heat flux, subcooled liquid temperature, saturation temperature of boiling liquid and pressure drop. The tube wall temperature gradient was measured using a set of ten K-type thermocouples, soldered directly to the wall. All the data were collected automatically using PC computer with a data acquisition interface. The measuring system used a specially developed in-house software TERMOLAB 06. From the test section the medium went to the



water cooled condenser and back to the main storage tank. The unit is also equipped with the filter/dryer and an additional pre-heater in the main tank (to be accomplished using hot water). The strong emphasis was put on the precision of temperature measurements, especially in the light of the fact that in some cases small wall – liquid temperature differences were encountered. The K type of sheathed thermocouples were used for the measurements of working medium temperature and the K type thermocouple wire was used for the wall temperature measurements. To maximize the accuracy above the standard values quoted by the producer, a special data acquisition interface – TERMOLAB 06 - was designed which ensured accuracy of ± 0.1 °C for the measuring range 0 - 120 °C and ± 0.3 °C for the range 120 - 300 °C. Additionally, each thermocouple was individually calibrated. It was carried out using the stabilized temperature at the accuracy not worse than ± 0.05 °C. Next, the whole system was tested in 3 constant temperature points: 0, 20 and 100 °C. This confirmed the average accuracy of temperature measurement at the level of ± 0.1 °C for each measuring channel. Maximum deviation between the 10 points on the tube length was also checked in the adiabatic single phase flow conditions and it amounted to ± 0.3 °C. This value can be admitted as a binding temperature measurement accuracy in the whole experiment.

Input power supplied to the test section (and further - the heat flux) was obtained by multiplying voltage measured on the tube length and current in the tube supplying circuit. Both measurements were carried out using digital multimeters M 890 G, whereas the current was measured in the shunt. The deviation of voltage measurement on the tube length was ± 0.8 % for the range 20 V AC (resolution 10 mV). The deviation of voltage measurement on the shunt was also ± 0.8 % for the range 2 V AC (resolution 1 mV). An error of the shunt resistance measurement and its characteristic determination was assessed as ± 1 %. The general error of input power measurements is about ± 3 % for the power of about 230 W.

The accuracy of obtained data was assumed by performing an uncertainty analysis based on the method of sequential perturbation (Moffat [11]). This method provides means to estimate the overall uncertainty of data by integrating the uncertainties of individual sources of error into the data base independently, then using a root-sum-square method to calculate the overall uncertainty. Error analysis was performed for every test run of each data set. It was executed automatically by implementing the above procedures in the data reduction spreadsheet. The heat balance was also automatically tested using: temperature difference and heat capacity for the case of single-phase heat exchange and enthalpy difference for the case of flow boiling.

The average error of heat transfer coefficient determination not exceeded 5 %. An error of pressure drop measurements for the case of single phase flow was on the level of 400 mbar. The distribution of the rate of heat imbalance against average quality is presented in Fig. 2. The fitting curve was considered in calculations to minimize the error of heat transfer coefficient determination.

EXPERIMENTAL RESULTS

In the investigations presented below the focus was set on the following issues:

1. Identification of dominant heat transfer mechanisms in minichannels.
2. Relations of heat transfer in two-phase flow in minichannels with respect to mass flow rate and heat flux, as well as channel diameter and variation with quality.
3. Comparison of data describing heat transfer with existing correlations for conventional and small diameter tubes.

The range of conditions studied in saturated flow boiling of R123 for upward flow in a vertical tube is presented in Table 1.

Prior to all tests the single phase heat transfer coefficient was calculated from the measurements. The results are presented in Fig. 3. Over 100 readings were taken to elaborate that test. The results were compared with the Dittus-Boelter [12] and Petukhov [13] correlations. None of the correlations exhibits full consistency with experiments. Better agreement is shown with the Dittus-Boelter correlation in case of the tube diameter $D=1.15\text{mm}$ and with Petukhov for $D=1.4\text{mm}$. All data are within the error band of $\pm 10\%$.

The effect of mass flux and heat flux

Figure 4 presents a qualitative distribution of heat transfer coefficient which has been observed during some of the experiments in literature, see for example Bar-Cohen and Rahim [10]. In flow boiling in conventional size channels there is observed a maximum in heat transfer coefficient distribution as a function of quality which is found at about $x \approx 0.8$. That location corresponds to the existence of annular flow structure in the tube. In studies of flows in minichannels there can also exist an additional maximum of heat transfer coefficient in its distribution as a function of quality, see Fig. 5. Similar findings were also found in the present study.

The mechanism of development of M-shape distribution can be explained in the following way. Values of heat transfer coefficient gradually increase from the values which are obtained at small subcoolings to the local maximum close to $x=0$. Then, the decrease is observed followed by a plateau and subsequently by a slight increase of heat transfer coefficient. The decrease of heat transfer coefficient maybe the result of suppression of nucleate boiling. That has also been confirmed by recent research by Thome [14], who confirms that the bubbly



flow is found in small diameter channels only up to qualities not exceeding $x \leq 0.1$. At values of quality about 60% the second maximum is observed. After that another decrease of heat transfer coefficient is found. The smallest values are reached when quality approaches 1, which is generally related to the dryout conditions. The M-shape distribution of heat transfer coefficient seems to be a specific phenomenon devoted merely to two-phase flows in minichannels. Initiation of boiling on the wall and related to it acceleration of saturated liquid flow induces significant rise of heat transfer coefficient, significantly above the level of single phase values. That may explain the first steep rise on the heat transfer coefficient distribution. Subsequent transition to the slug/plug flow structure renders gradual decrease of heat transfer coefficient, as the vapour slugs form conditions for local evaporation of thin liquid film, separating the liquid and the wall, and even to development of dry patches, which impair heat transfer. The transition to annular flow structure again results in increase of heat transfer coefficient, as a result of development of evaporating thin liquid film on the wall. The evaporating film thins and splits into rivulets causing local dryout conditions. The experimental evidence available in literature refer to a smaller range of quality and enable to reflect only a part of the M-shaped curve. Detailed analysis of experimental data enables to conclude that different sets of data describe different parts of M-shape distributions. That is the reason why in some cases authors are claiming the reduction of heat transfer coefficient with quality and some – the increasing trend.

From Figures 6 to 8 it can be clearly seen that the local heat transfer coefficient depends on heat flux at a set values of mass velocity. These data have been collected for the tube diameters of 2.3 mm. In Fig. 9 and 10 presented are data for the smaller tube size, i.e. $d=1.15$ mm. The relation is however not very straightforward. Because of quite big dispersion of experimental data the trend lines are introduced to connect the appropriate labels



corresponding to the same heat flux to make them more legible. Strong non-equilibrium character of the process can be the reason for this dispersion, however presented data have been repeated several times for the specified inlet conditions (at least 20 times). Values of heat transfer coefficient vary non-monotonically with quality, showing up the presence of the first peak in heat transfer distribution at lower qualities. The highest absolute value of the peak is found for the smallest heat flux at a specified mass velocity. Following the reduction of heat transfer coefficient and a subsequent plateau the increase in all cases is observed. That increase leads probably to the second peak. In case of smaller tube sizes the peak is found for smaller values of quality than in case of larger tubes, see Fig. 9 and 10.

Now we can turn our attention to the case where we have distributions of heat transfer coefficient with respect to quality at set values of heat flux and varying mass velocity. Figures 11 to 13 show the measured distributions of heat transfer coefficient for such conditions for the tube size of 2.3 mm, whereas in Fig. 14 and 15 presented are results for the smaller tube size. The results of experimental investigations presented in these figures clearly show two maxima on the heat transfer coefficient with respect to quality, namely the first one at qualities around 0.1 - 0.2 and the second one at qualities around 0.6 - 0.8. In these cases the trends in the development of peaks is much clearer than in the previous case where at constant mass velocity the heat flux varied. At a constant value of heat flux the most shifted to high qualities peak in heat transfer coefficient corresponds to the lowest value of mass velocity. That maximum is revealed at values of quality equal about 0.8. The absolute value of the peak is also the highest in such case, i.e. smallest mass velocity. Following subsequent increase of mass velocity we can observe the peak developing at small qualities. With increasing mass velocities the peak shifts left and reduces its maximum value. That peak corresponds to the value of quality of about 0.1. The difference between absolute values of both maxima is quite

significant, as the second maximum can be reaching a twice higher value than the first one. In our opinion, similarly to the knowledge from conventional channels, the first maximum arises as a result of suppression of nucleate boiling. Another mechanism is present in the case of the second maximum. The second peak is caused by the fact that the annular film is drying up. As long as the surface is wet (in annular flow) the heat transfer coefficient is increasing due to the thinning of the liquid annular film. When the film breaks down the heat transfer coefficient decreases rapidly. Heat transfer coefficient values at the maximum are bigger for the inner diameter of 1.15 mm than for 2.3 mm, see Fig. 14 to 15.

Comparison with correlation due to Mikielewicz and co-workers [15,16]

Figures 16 and 17 present collected experimental results compared with theoretical values determined from the model due to Mikielewicz and co-workers [15,16], which devises how to calculate the heat transfer coefficients in flow boiling from the following formulae:

$$\frac{\alpha_{TPB}}{\alpha_L} = \sqrt{R_{MS}^n + \frac{1}{1 + 2.53 \times 10^{-3} \text{Re}^{1.17} \text{Bo}^{0.6} (R_{MS} - 1)^{-0.65}} \left(\frac{\alpha_{PB}}{\alpha_L} \right)^2} \quad (1)$$

The pool boiling heat transfer coefficient α_{PB} , is to be calculated from the relation due to Cooper [17]. The two-phase flow multiplier R_{MS} due to Müller-Steinhagen and Heck [18] is recommended for use in case of refrigerants, Ould Didi et al. [19]. The R_{MS} acts in the correction as a sort of convective number, known from other correlations. In the form applicable to small diameter channels the modified Muller-Steinhagen and Heck model yields:

$$R_{MS} = \left[1 + 2 \left(\frac{1}{f_1} - 1 \right) x \text{Con}^m \right] \cdot (1-x)^{1/3} + x^3 \frac{1}{f_{1z}} \quad (2)$$

where $\text{Con} = (\sigma/g/(\rho_L - \rho_G))^{0.5}/d$. Best consistency with experimental data has been obtained for $m = -1$, Mikielwicz and co-workers [15,16]. In (2) $f_1 = (\rho_L/\rho_G) (\mu_L/\mu_G)^{0.25}$ for turbulent flow and $f_1 = (\rho_L/\rho_G)(\mu_L/\mu_G)$ for laminar flows, whereas $f_{1z} = (\mu_G/\mu_L)(\lambda_L/\lambda_G)^{1.5}(C_{pL}/C_{pG})$ for turbulent flows and $f_{1z} = (\lambda_G/\lambda_L)$ for laminar flows. The applied heat flux is incorporated through the boiling number Bo , defined as, $\text{Bo} = q/(Gh_{LG})$. In case of turbulent flow exponent n assumes a value of 0.9, whereas in case of laminar flow that exponent assumes a value of $n = 2$. It appears that over 65% of measurements is contained in $\pm 30\%$ error limits and 85% is contained in $\pm 50\%$ error limits. This error spreads regularly for each quality value (Fig. 17). The biggest discrepancy appears for high values of quality. It follows that the correlation (1) over predicts values the heat transfer coefficient for high qualities.

Comparison with other empirical correlations

There are many correlations for saturated flow boiling available in the literature. Many of such correlations work well mainly with authors own data but they fail to reproduce correctly other authors data. Results of the comparisons of the present experimental data with the correlation described by expression (1) are presented in Figures 18 and 19. Three correlations from the literature were used, which are adequate for flow boiling in mini- and microchannels. These are correlations due to Kandlikar and Steinke [20], Lazarek and Black [1] and Owhaib [21]. Although the tested range of parameters in the presented work corresponded to the higher values of mass velocity these empirical correlations have been selected for comparisons just to be able to perform any tests with other experimental data. The

experimental conditions selected for comparison here were just outside the range of applicability of the correlations from literature but there are no other well established correlations available for the range of parameters considered here. Results calculated from these correlations were compared with the results of calculations obtained using correlation (1). Supremacy of the Mikielewicz and co-workers [15,16] correlation over the other correlations used in this work to describe heat transfer in minichannels can be noticed. Practically other correlations describe the experimental data properly only in few cases. In Figures 20 and 21 presented are also calculations using authors own method applied to the data due to Karayiannis [9]. It is apparent from Fig. 16 that the discrepancies exceeding 30% are visible only for the quality close to zero. All other data fall into the envelope of $\pm 30\%$. That result must be deemed satisfactory. Another experimental set of data against which the correlation was tested were data due to Bao et al. [8] and Wambsganns et al. [4]. Also here satisfactory comparisons have been obtained, see Fig. 22 and 23.

Two-phase flow visualization

Images of the flow patterns were registered using a high speed CCD camera at exposure time of $32\mu\text{s}$ on a 9 mm tube segment (starting from 30-th cm of total tube length, i.e. corresponding to the tube outlet). Recording was carried out at a constant values of heat flux $q = 39.7 \text{ kW/m}^2$ and variable mass velocity. A special two-segment test section was used. First segment, made of silver tube with 2.3 mm internal diameter, was used to heat the liquid to the required parameters. In the second segment, made of quartz glass with the same inner diameter, flow boiling was continued adiabatically and recorded under such conditions. Known flow structures of the flow were captured, which are presented in Figures 24 to 27.

CONCLUSIONS

This work partly explains the specific features of two-phase flow and heat transfer inside minichannels. Within the framework of experimental and theoretical works authors realised the following observations:

Qualitatively and quantitatively different patterns of heat transfer coefficient in function of quality were detected. In a general case two maximum values of heat transfer coefficient as a function of quality can be found. The first one occurs at the small vapour content in the flow in minichannel (quality of about 0.1). In most other authors experiments the decreasing heat transfer coefficient character was noticed because most of the measurements were executed for $0.1 < x < 0.7$, which is before attaining the second heat transfer coefficient maximum conditions. That maximum was noticed for some flow parameters (for bigger qualities, $x \approx 0.7 - 0.8$). Presence of these two maxima leads to the “M-shape” distribution of heat transfer coefficient. This observation was identified only recently in the literature [10]. Heat transfer coefficient increase with decreasing tube diameter was also shown in the some quality range. Also noticed was the fact, that heat transfer coefficient maximum values are bigger for the smaller channel diameters.

Comparison of experimental data with some correlations from literature show that the correlation due to Mikielewicz [16] returns best consistency of those selected for comparisons here. Other correlations are satisfactory only in selected cases.

ACKNOWLEDGEMENTS

The reported work has been partially funded from the research projects of the Ministry for Science and Higher Education 3T10B 074 29, 3T10B 071 29 and N512 4590 36.

NOMENCLATURE

$Bo = \frac{q \cdot l \cdot \rho_L}{\rho_G \cdot h_{LG} \cdot \mu_L}$	- Boiling number
C	- specific heat
C_p	- specific heat at constant pressure, J/kgK
d	- channel inner diameter, m
L	- channel length, m
f	- function in equation (2)
g	- gravity, m/s ²
G	- mass flowrate, kg/m ² s
h	- enthalpy, J/kg
h_{LG}	- latent heat of evaporation, J/kg
l	- bubble characteristic length, channel length, m
m	- parameter in equation (2)
n	- parameter in equation (1)
p	- pressure, Pa
$Pr = \frac{\mu_L \cdot C_L}{\lambda_L}$	- Prandtl number
q	- heat flux density, W/m ²
R_{ms}	- two-phase flow multiplier
$Re = \frac{G \cdot d}{\mu_L}$	- Reynolds number



t - temperature, °C

x - quality

Greek symbols

α - heat transfer coefficient, W/m²K

λ - thermal conductivity, W/mK

μ - dynamic viscosity, Pa s

ρ - density, kg/m³

σ - surface tension, N/m

Subscripts

G - saturated vapour

i - internal

in - inlet

L - saturated liquid

PB - pool boiling

SAT - saturation conditions

sub - subcooled

TPB - two-phase boiling

w - wall

REFERENCES

- [1] Lazarek, G.M., Black, S.H., *Evaporative heat transfer, pressure drop and critical heat flux in a small vertical tube with R-113*, Int. J. Heat Mass Transfer, Vol. 25, No. 7, pp. 945-960, 1982. (article)
- [2] Chen, J.C., Correlation for boiling heat-transfer to saturated fluids in convective flow, Ind. Chem. Eng. Proc. Des. Dev, Vol. 5, No. 3, pp. 322-339, 1966. (article)
- [3] Shah, M.M., A new correlation for heat transfer during boiling flow through pipes, ASHRAE Trans., Vol. 82, part 2, pp. 66-86, 1976. (article)
- [4] Wambsganss, M.W., France, D.M., Jendrzejczyk, J.A., Tran, T.N., *Boiling heat transfer in a horizontal small-diameter tube*, Journal of heat transfer, Vol. 115, pp. 963-972, 1993. (article)
- [5] Tran, T.N., Wambsganss, M.W., France, D.M., Small circular- and rectangular-channel boiling with two-phase refrigerants, Int. J. Multiphase Flow, Vol. 22, No. 3, pp. 485-498, 1996. (article)
- [6] Tran, T.N., Wambsganss, M.W., Chyu, M.C., France, D.M., *A correlation for nucleate flow boiling in small channels*, In: Shah, R.K. (Ed), Compact Heat Exchanger for the Process Industries. Begell House, New York, pp. 353-363, 1997. (book)
- [7] Kew, P., Cornwell, K., *Correlations for the prediction of boiling heat transfer in small diameter channels*, Applied Thermal Engineering, Vol. 17, pp. 705-715, 1997. (article)
- [8] Bao, Z.Y., Fletcher, D.F., Haynes, B.S., *Flow boiling heat transfer of R11 and HCFC123 in narrow passages*, Int. J. Heat Mass Transfer, Vol. 43, pp. 3347-3358, 2000. (article)
- [9]. Huo, X., Chen, L., Tian, Y.S., Karayiannis, T.G., Flow boiling and flow regimes in small diameter tubes, Applied Thermal Engineering, Vol. 24 pp. 1225-1239, 2007. (article)
- [10] Bar-Cohen, A., Rahim, E., *Modeling and prediction of two-phase microgap channel heat transfer characteristics*, Heat Transfer Engineering, Vol. 30, No. 8, pp. 601-625, 2009. (article)



- [11] Moffat, R.J., *Describing the uncertainties in experimental results*, Experimental thermal and fluid science, Vol. 1, pp. 3-17, 1988. (article)
- [12] Dittus, F.W., Boelter, L.M.K., Heat transfer in automobile radiators of tubular type, University of California Pub. Eng., 2, pp. 443-461, 1930. (article)
- [13] Petukhov, B., Kurganov, V.A., Gladuntsov, A.I., Heat transfer in turbulent pipe flow of gases with variable properties, Heat Transfer Soviet Research, Vol. 5, pp. 109-116, 1973. (article)
- [14] Thome, J.R., Chapter I, Wolverine Engineering Databook III, at www.wlv.com/products, 2007. (electronic book)
- [15] Mikielwicz, D., Mikielwicz, J., Tesmar, J., *Improved semi-empirical method for determination of heat transfer coefficient in flow boiling in conventional and small diameter tubes*, Int. J. of Heat and Mass Transfer, Vol. 50, pp. 3949-3956, 2007. (article)
- [16] Mikielwicz, D., *A New Method for Determination of Flow Boiling Heat Transfer Coefficient in Conventional-Diameter Channels and Minichannels*, Heat Transfer Engineering, Vol. 31, No. 4, pp. 276-284, 2009. (article)
- [17] Cooper, M. G., *Saturation nucleate pool boiling: a simple correlation*, Int. Chem. Eng. Symposium 1, Vol. 86, pp. 785-793, 1984. (article)
- [18] Müller-Steinhagen, R., Heck, K., *A simple friction pressure drop correlation for two-phase flow in pipes*, Chem. Eng. Progress, Vol. 20, 1986. (article)
- [19] Ould Didi, M.B., Kattan, N., Thome, J.R., Prediction of two-phase pressure gradients of refrigerants in horizontal tubes, Int. J. of Refrigeration, Vol. 25, pp. 935-947, 2002. (article)
- [20] Steinke, M., Kandlikar, S., *An experimental investigation of flow boiling characteristics of water in parallel microchannels*, Journal of Heat Transfer, Vol. 126, No. 4, pp. 518-526, 2004. (article)



[21] Owhaib, W., *Experimental heat transfer, pressure drop and flow visualization of R134a in vertical mini/micro tubes*, PhD Thesis, KTH, Stockholm, 2007. (book)

Table 1. Range of variation of parameters in investigations of flow boiling of R123.

<i>Parameter</i>	<i>Range of variation</i>
d_i [mm]	1.15, 2.3
G [kg/(m ² s)]	534 - 3011
q_w [kW/m ²]	28.5 - 68.4
t_{SAT} [°C]	23 - 86
x [--]	0 - 1
L [mm]	380

Figure captions:

Fig. 1. Schematic of experimental assembly: 1- main tank with pre-heater; 2 – circulation pump; 3 – filter and dryer; 4 – mass flow meter; 5 – pre-heater; 6 – test section; 7 – condenser; 8 – by-pass; 9 – filling in valve; 10 – de-aerator / vacuum pump valve.

Fig. 2. Distribution of rate of heat imbalance against the average quality.

Fig. 3. Single phase convection for two tube sizes with R123 as a test fluid.

Fig. 4. Heat transfer distribution in conventional size channel and minichannels

Fig. 5. Schematic of M-shape distribution of heat transfer coefficient minichannels

Fig. 6. Distributions of heat transfer coefficient with respect to quality for fixed values of mass velocity and varying heat flux, $D=2.3$ mm, $G=950$ kg/(m²s).

Fig. 7. Distributions of heat transfer coefficient with respect to quality for fixed values of mass velocity and varying heat flux, $D=2.3$ mm, $G=2007$ kg/(m²s).

Fig. 8. Distributions of heat transfer coefficient with respect to quality for fixed values of mass velocity and varying heat flux, $D=2.3$ mm, $G=2550$ kg/(m²s).

Fig. 9. Distributions of heat transfer coefficient with respect to quality for fixed values of heat flux and varying mass velocity, $D=2.3$ mm, $q=48080$ W/m².

Fig. 10. Distributions of heat transfer coefficient with respect to quality for fixed values of heat flux and varying mass velocity, $D=2.3$ mm, $q=49246$ W/m².

Fig. 11. Distributions of heat transfer coefficient with respect to quality for fixed values of heat flux and varying mass velocity, $D=2.3$ mm, $q=58450$ W/m².

Fig. 12. Distributions of heat transfer coefficient with respect to quality for fixed values of mass velocity and varying heat flux, $D=1.15$ mm, $G=870$ kg/(m²s).

Fig. 13. Distributions of heat transfer coefficient with respect to quality for fixed values of mass velocity and varying heat flux, $D=1.15$ mm, $G=1070$ kg/(m²s).

Fig. 14. Distributions of heat transfer coefficient with respect to quality for fixed values of heat flux and varying mass velocity, $D=1.15$ mm, $q=22318$ W/m².

Fig. 15. Distributions of heat transfer coefficient with respect to quality for fixed values of heat flux and varying mass velocity, $D=1.15$ mm, $q=66500$ W/m².

Fig. 16. Experimental heat transfer coefficient as a function of heat transfer coefficient determined by expression (1), $D=2.3$ mm.

Fig. 17. Ratio of experimental heat transfer coefficient to a value calculated by expression (1) as a function of quality, $D=2.3$ mm.

Fig. 18. Comparison of obtained experimental data with other correlations for small diameter channel as a function of quality, $G=822$ kg/m²s, $q=59641$ W/m², $d=2.3$ mm.

Fig. 19. Comparison of obtained experimental data with other correlations for small diameter channel in function of quality, $G=824$ kg/m²s, $q=63620$ W/m², $d=2.3$ mm.

Fig. 20. Data due to Huo et al. [9] reduced with correlation (1).

Fig. 21. Data due to Huo et al. [9] versus quality reduced with correlation (1).

Fig. 22. Comparisons with experimental data due to Tran et al. [5] and Wambsganss et al. [4]

Fig. 23. Comparisons with experimental data due to Tran et al. [5] and Wambsganss et al. [4]

Fig. 24. Beginning of nucleate boiling, $q = 39,7$ kW/m², $G = 2883$ kg/m²s, $t_{in} = 22.51$ °C.

Fig. 25. Developed nucleate boiling, $q = 39,7$ kW/m², $G = 3650$ kg/m²s, $t_{in} = 30.75$ °C.

Fig. 26. Wispy-annular flow boiling, $q = 39,7$ kW/m², $G = 2237$ kg/m²s, $t_{in} = 41.53$ °C.

Fig. 27. Mist-annular flow boiling, $q = 39,7$ kW/m², $G = 783$ kg/m²s, $t_{in} = 54.09$ °C.

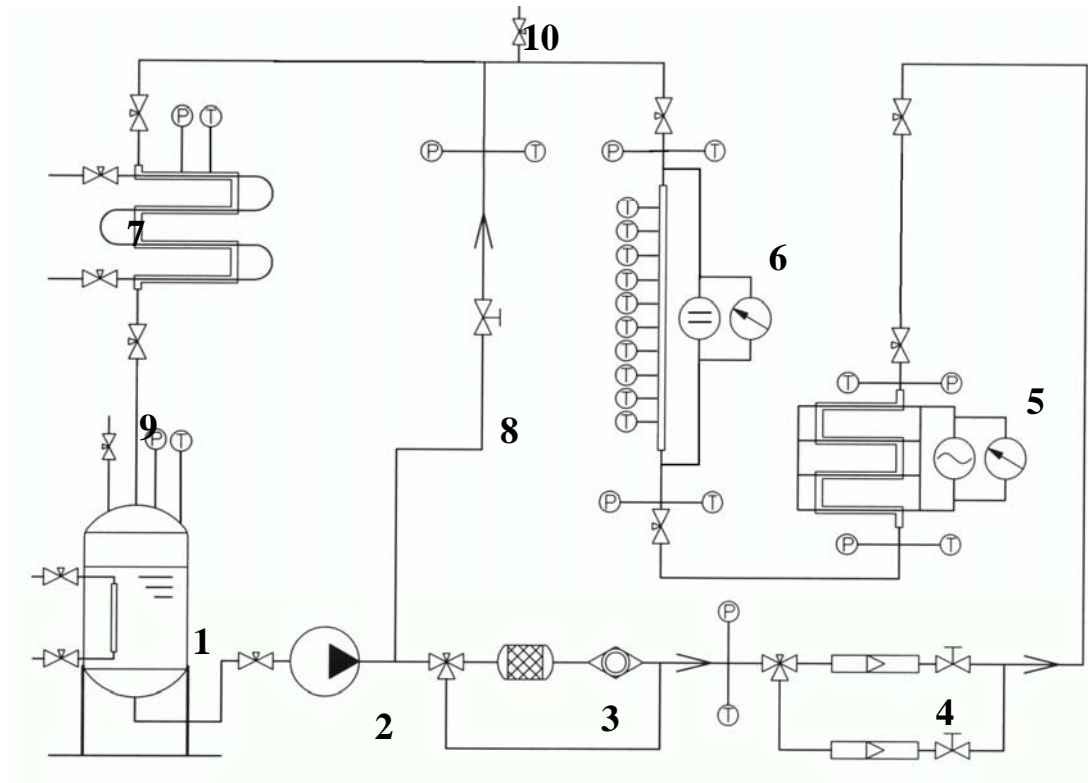


Fig. 1. Schematic of experimental assembly: 1- main tank with pre-heater; 2 – circulation pump; 3 – filter and dryer; 4 – mass flow meter; 5 – pre-heater; 6 – test section; 7 – condenser; 8 – by-pass; 9 – filling in valve; 10 – de-aerator / vacuum pump valve.

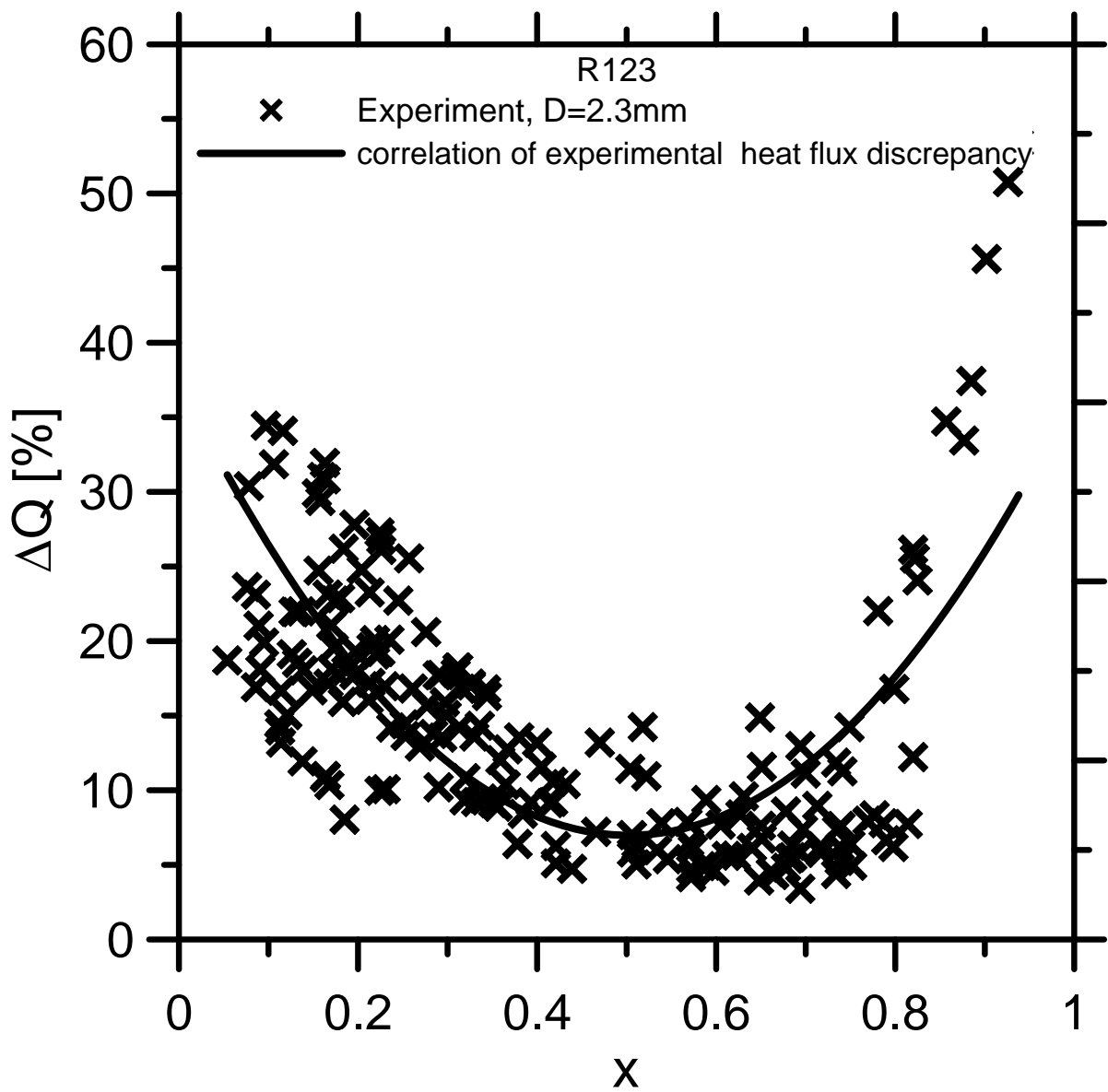


Fig. 2. Distribution of rate of heat imbalance against the average quality.

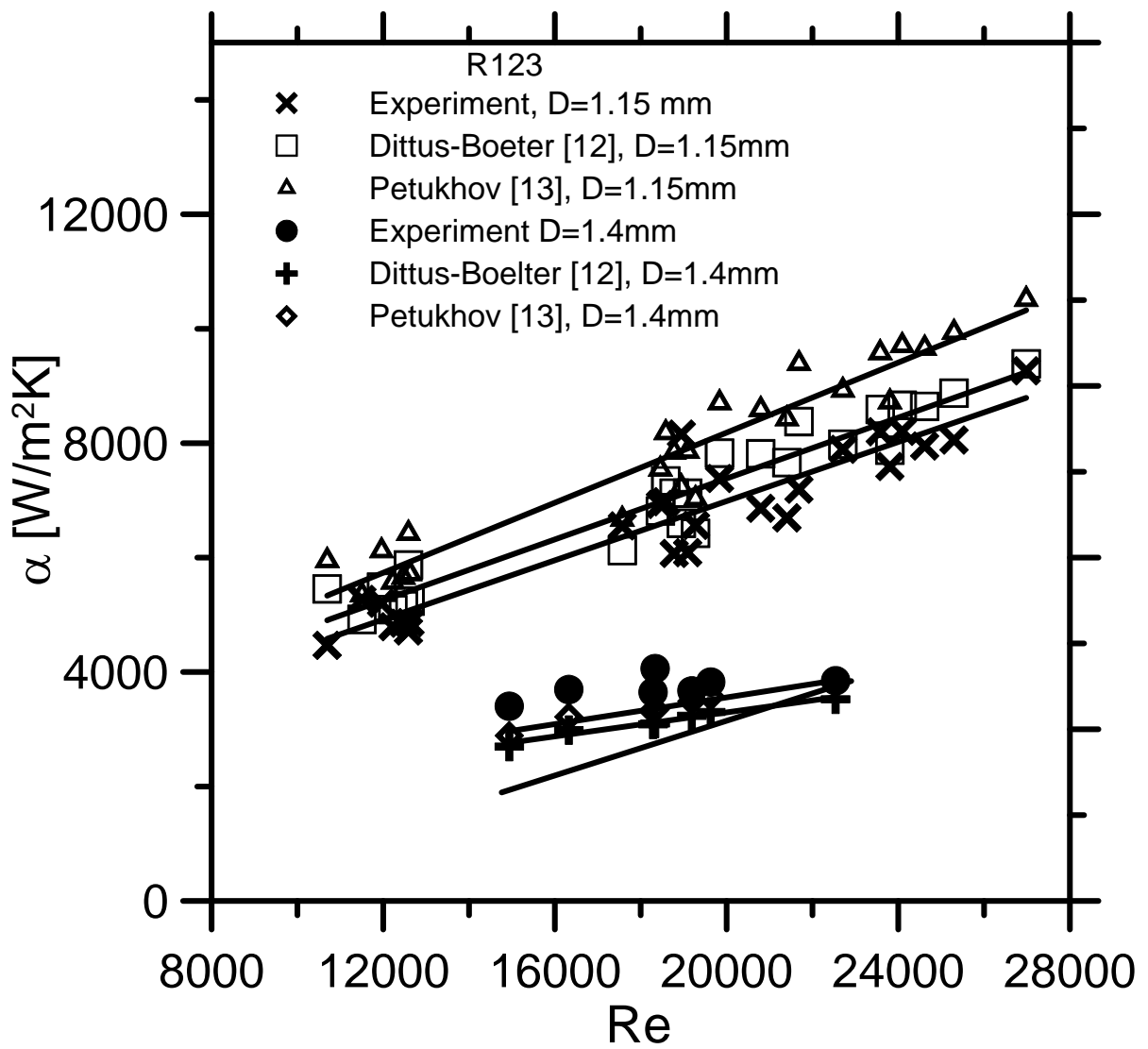


Fig. 3. Single phase convection for two tube sizes with R123 as a test fluid.

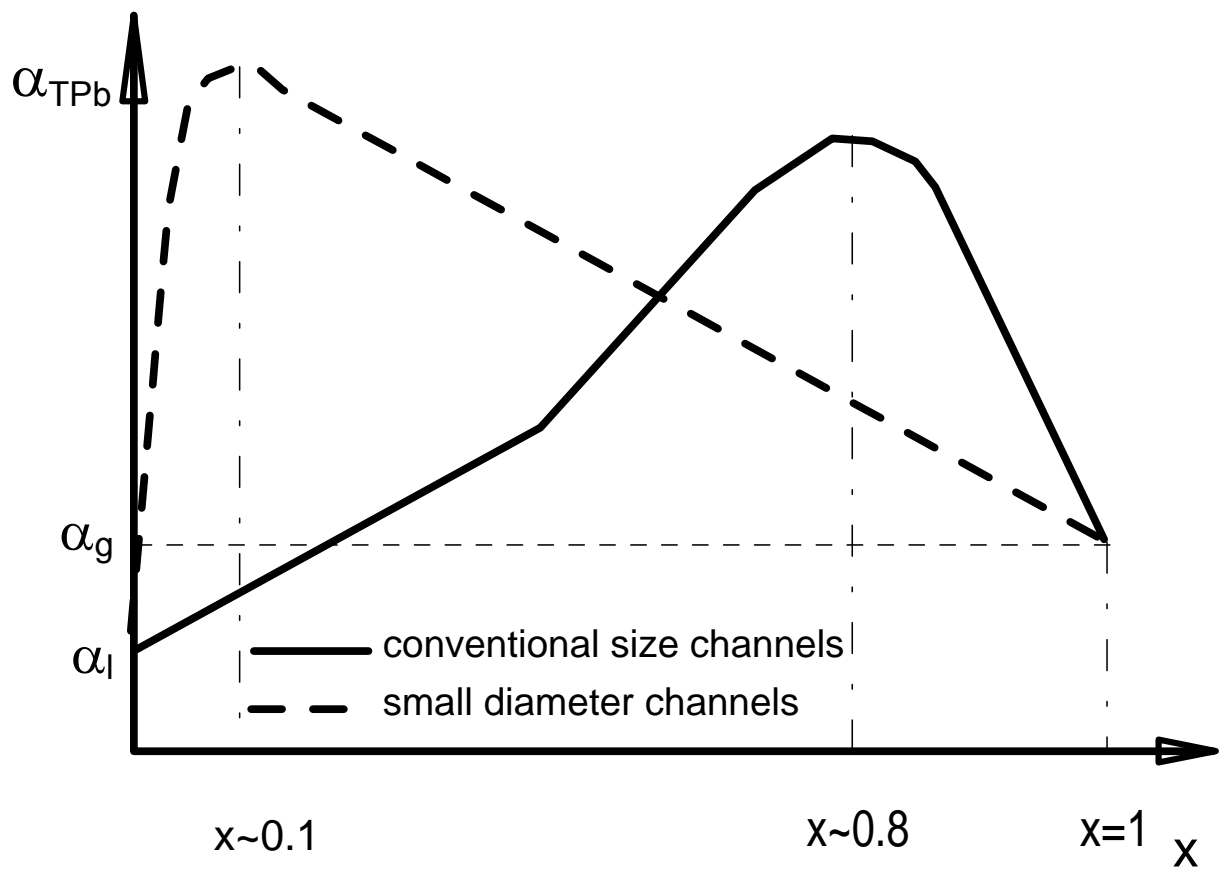


Fig. 4. Heat transfer distribution in conventional size channel and minichannels

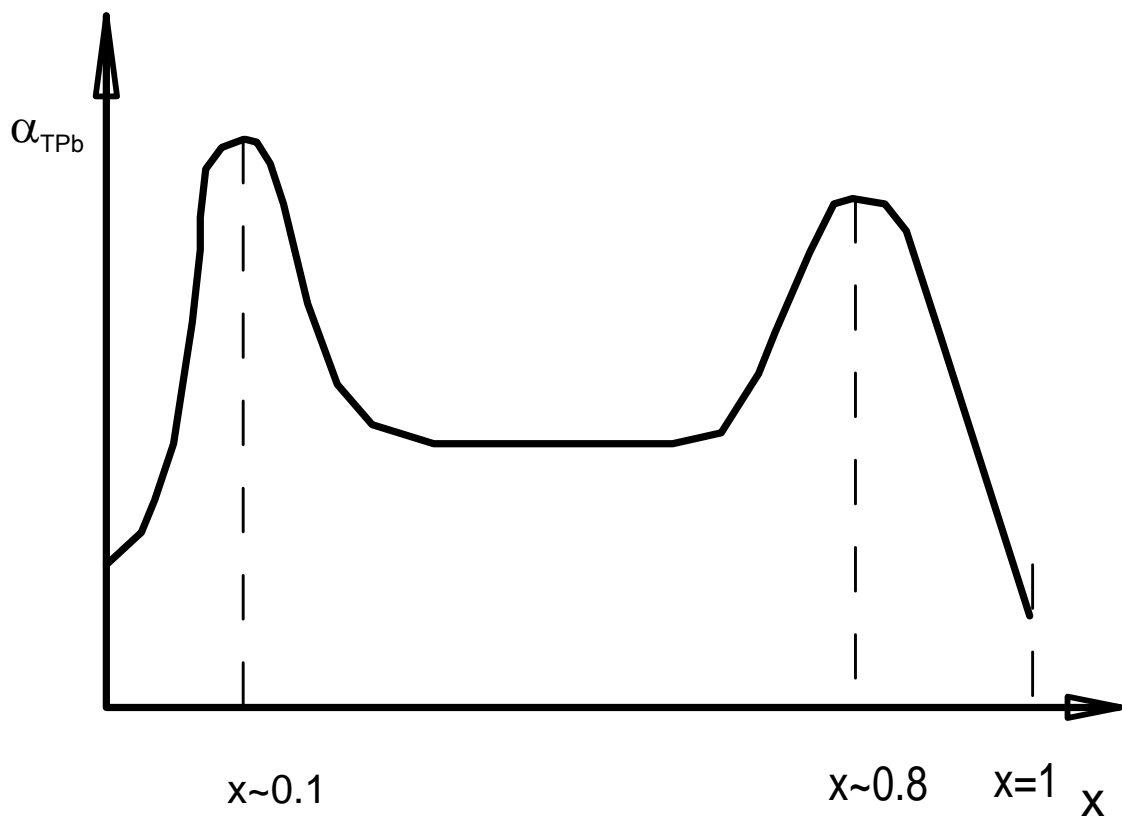


Fig. 5. Schematic of M-shape distribution of heat transfer coefficient minichannels

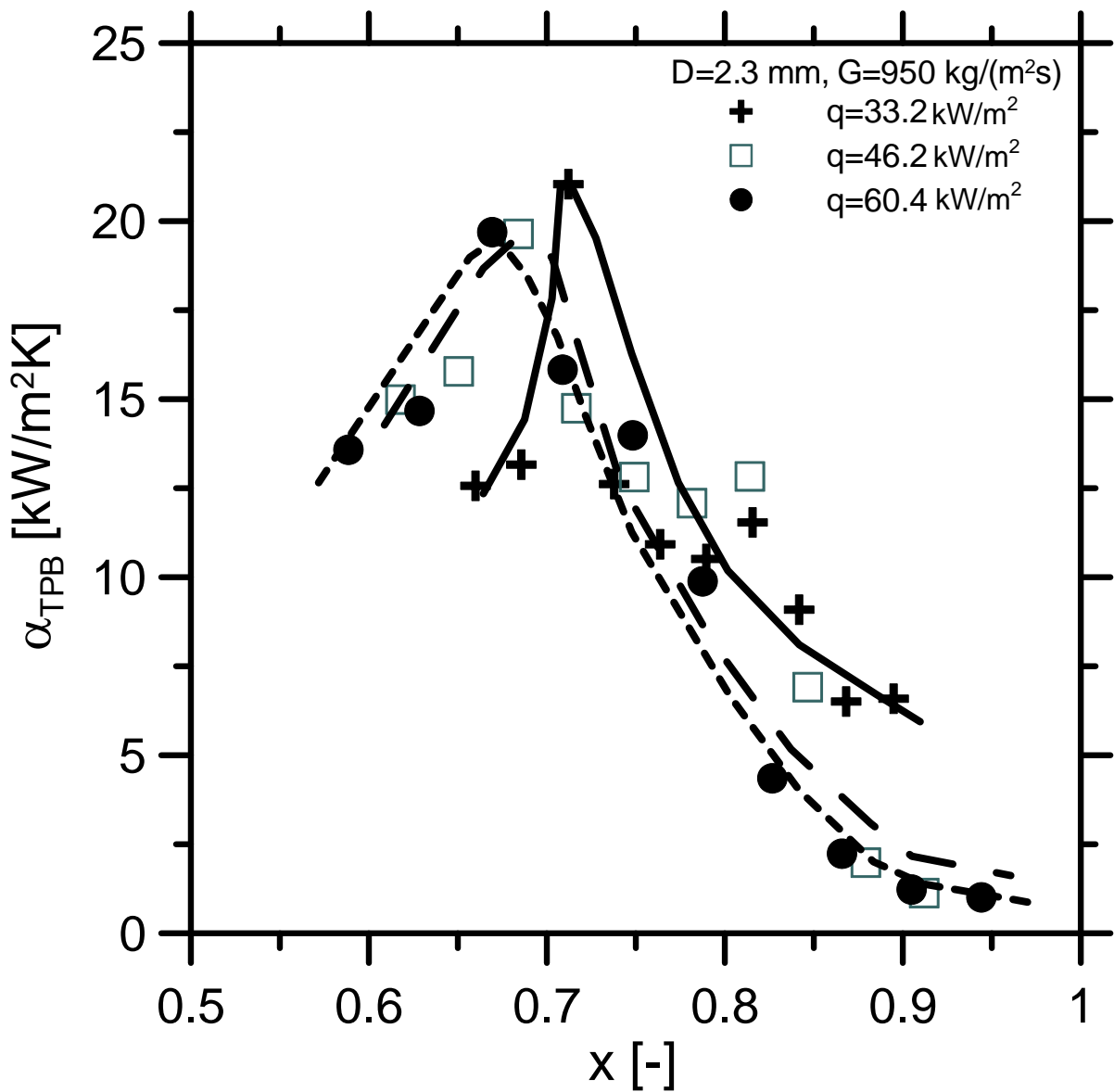


Figure 6. Distributions of heat transfer coefficient with respect to quality for fixed values of mass velocity and varying heat flux, $D=2.3 \text{ mm}$, $G=950 \text{ kg/(m}^2\text{s)}$.

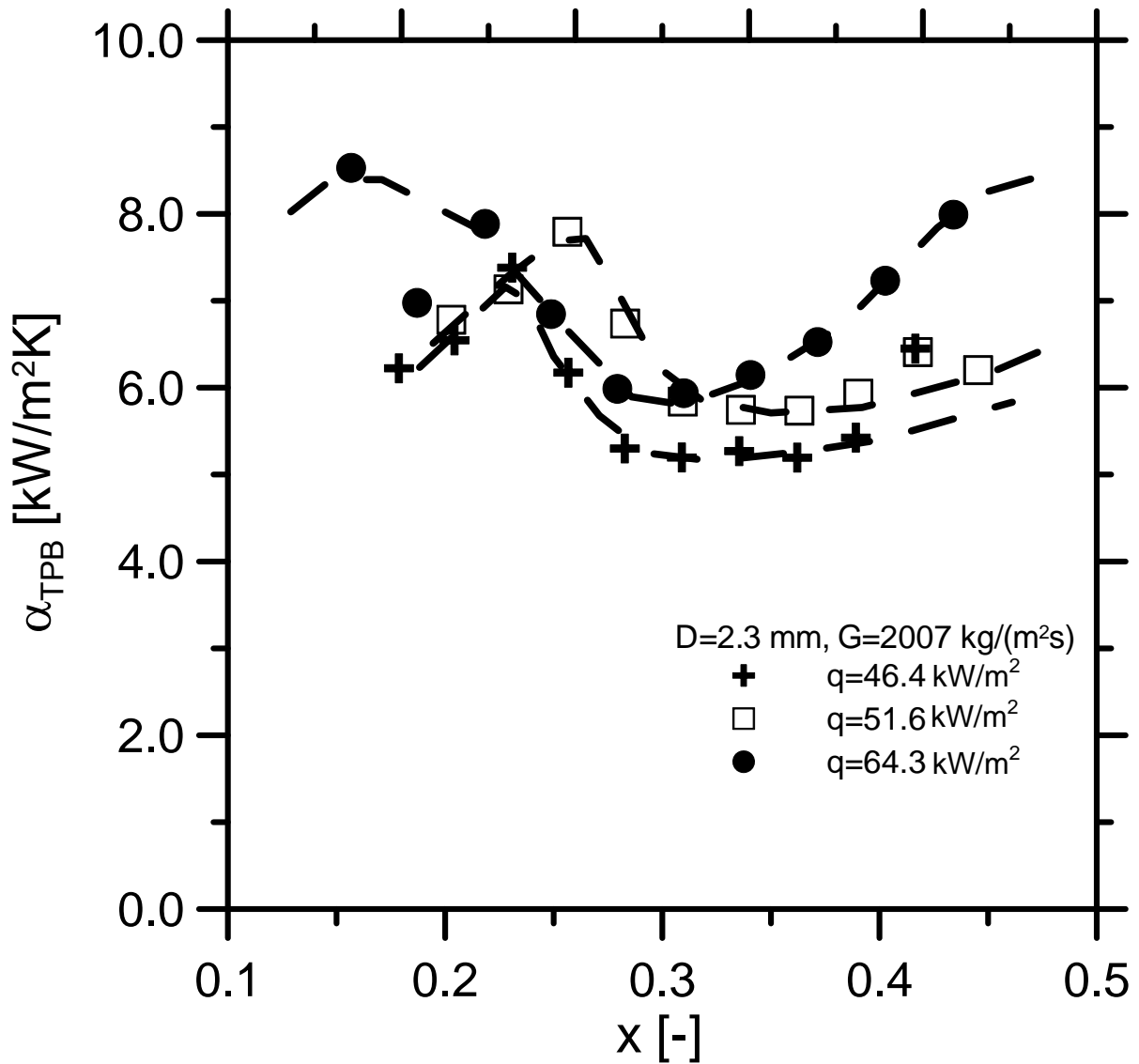


Figure 7. Distributions of heat transfer coefficient with respect to quality for fixed values of mass velocity and varying heat flux, $D=2.3 \text{ mm}$, $G=2007 \text{ kg}/(\text{m}^2\text{s})$.

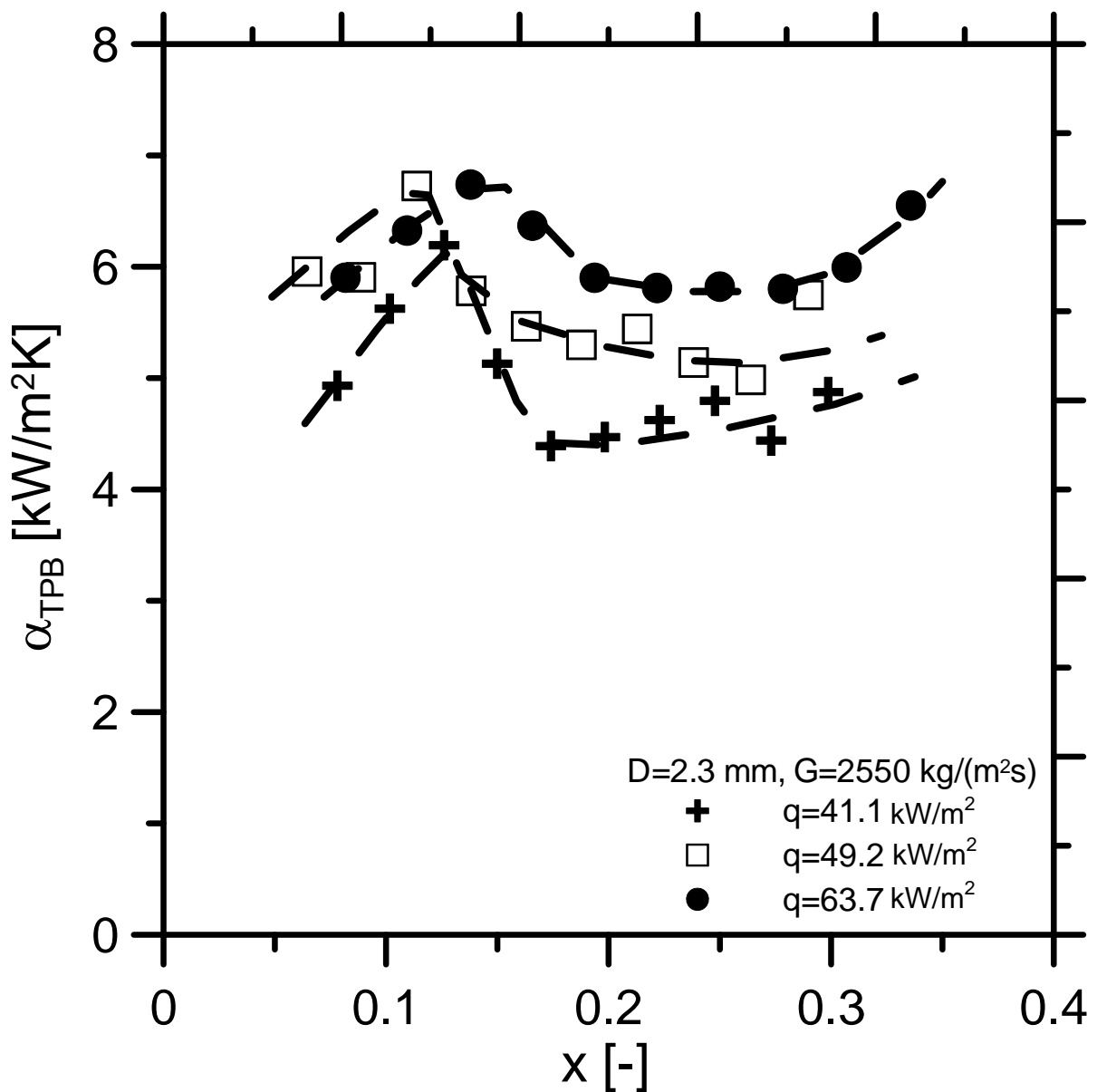


Figure 8. Distributions of heat transfer coefficient with respect to quality for fixed values of mass velocity and varying heat flux, $D=2.3 \text{ mm}, G=2550 \text{ kg}/(\text{m}^2\text{s})$.

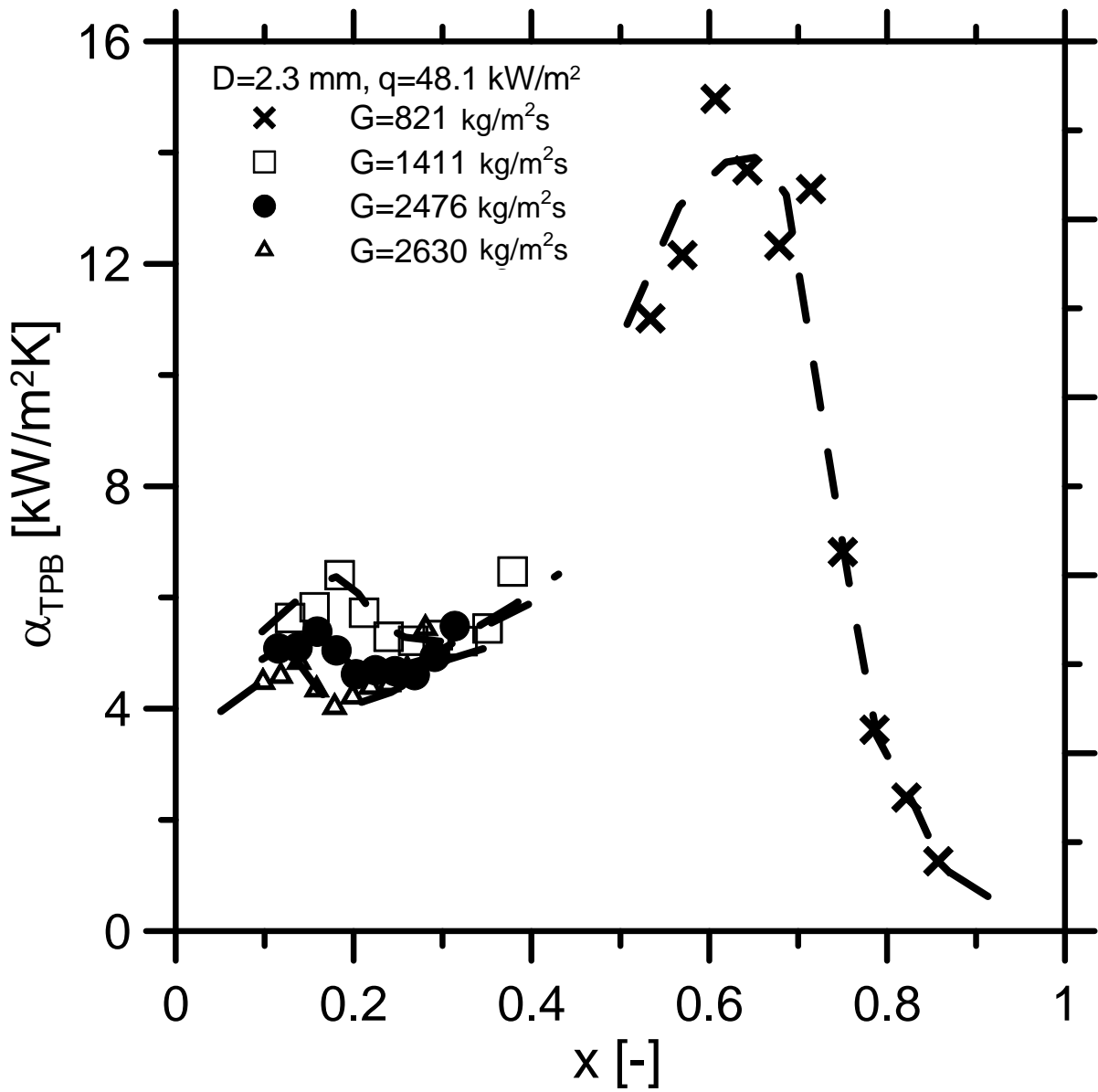


Figure 9. Distributions of heat transfer coefficient with respect to quality for fixed values of heat flux and varying mass velocity, $D=2.3 \text{ mm}, q=48080 \text{ W/m}^2$.

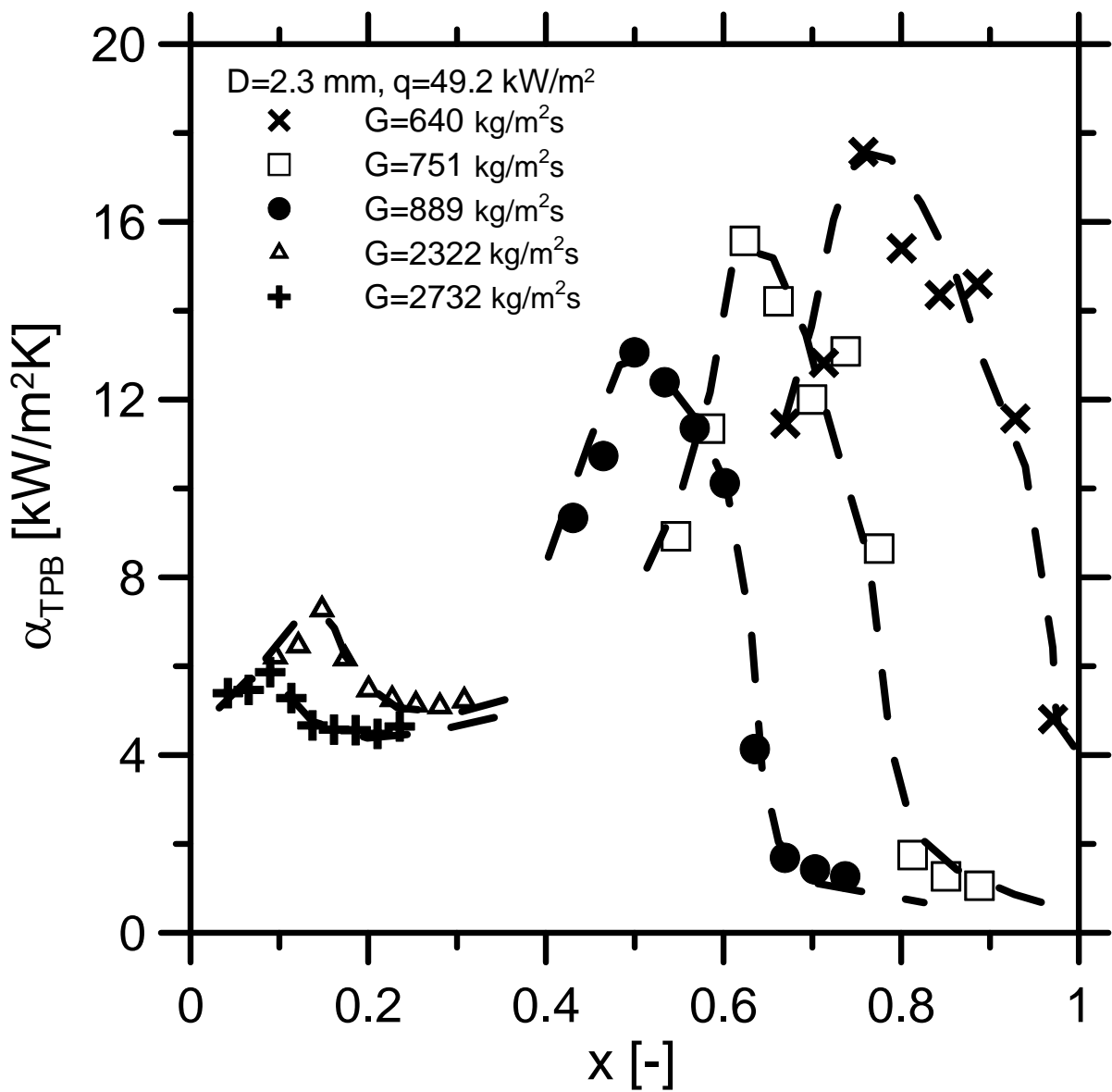


Figure 10. Distributions of heat transfer coefficient with respect to quality for fixed values of heat flux and varying mass velocity, $D=2.3 \text{ mm}, q=49246 \text{ W/m}^2$.

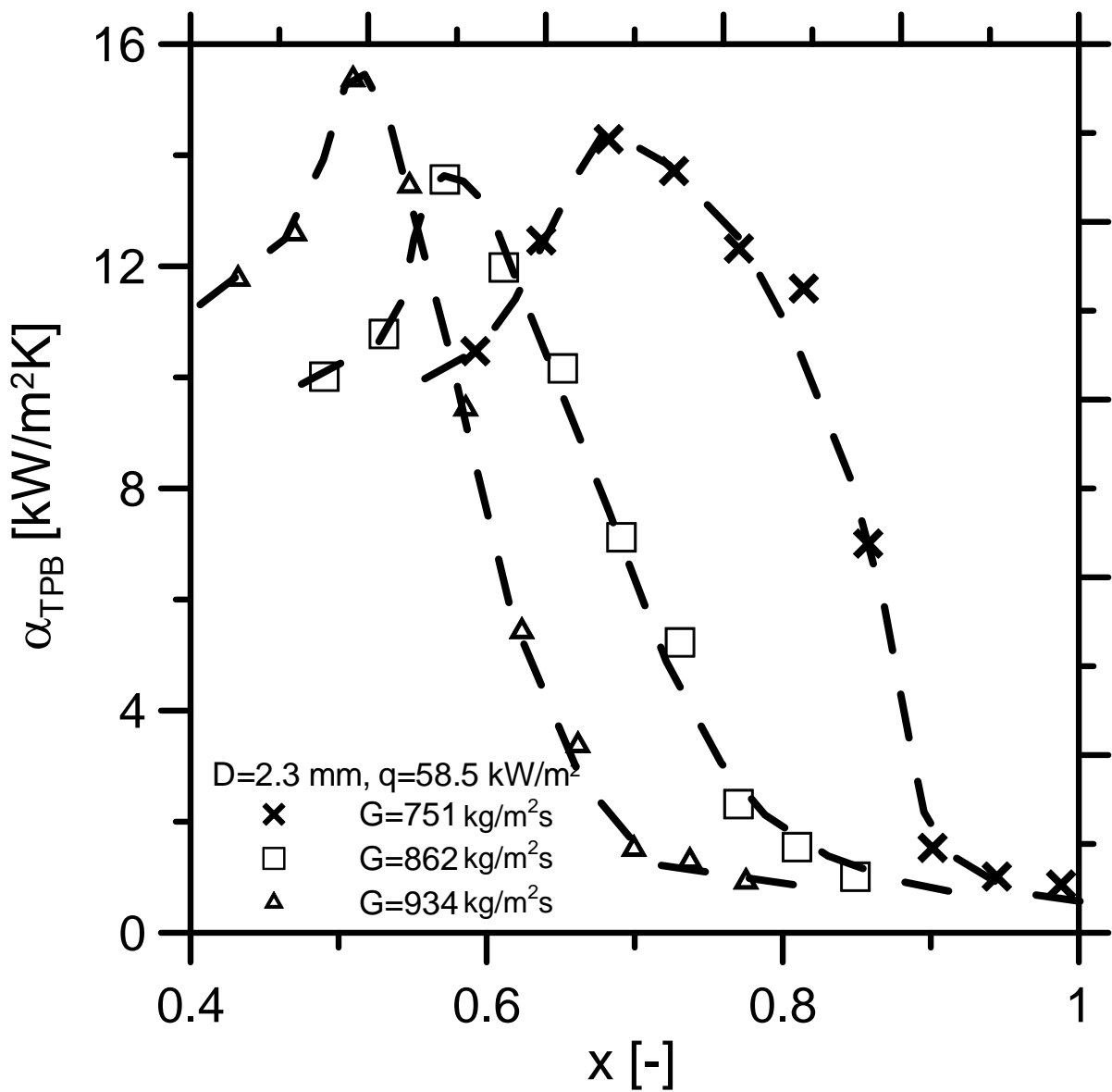


Figure 11. Distributions of heat transfer coefficient with respect to quality for fixed values of heat flux and varying mass velocity, $D=2.3$ mm, $q=58450$ W/m².

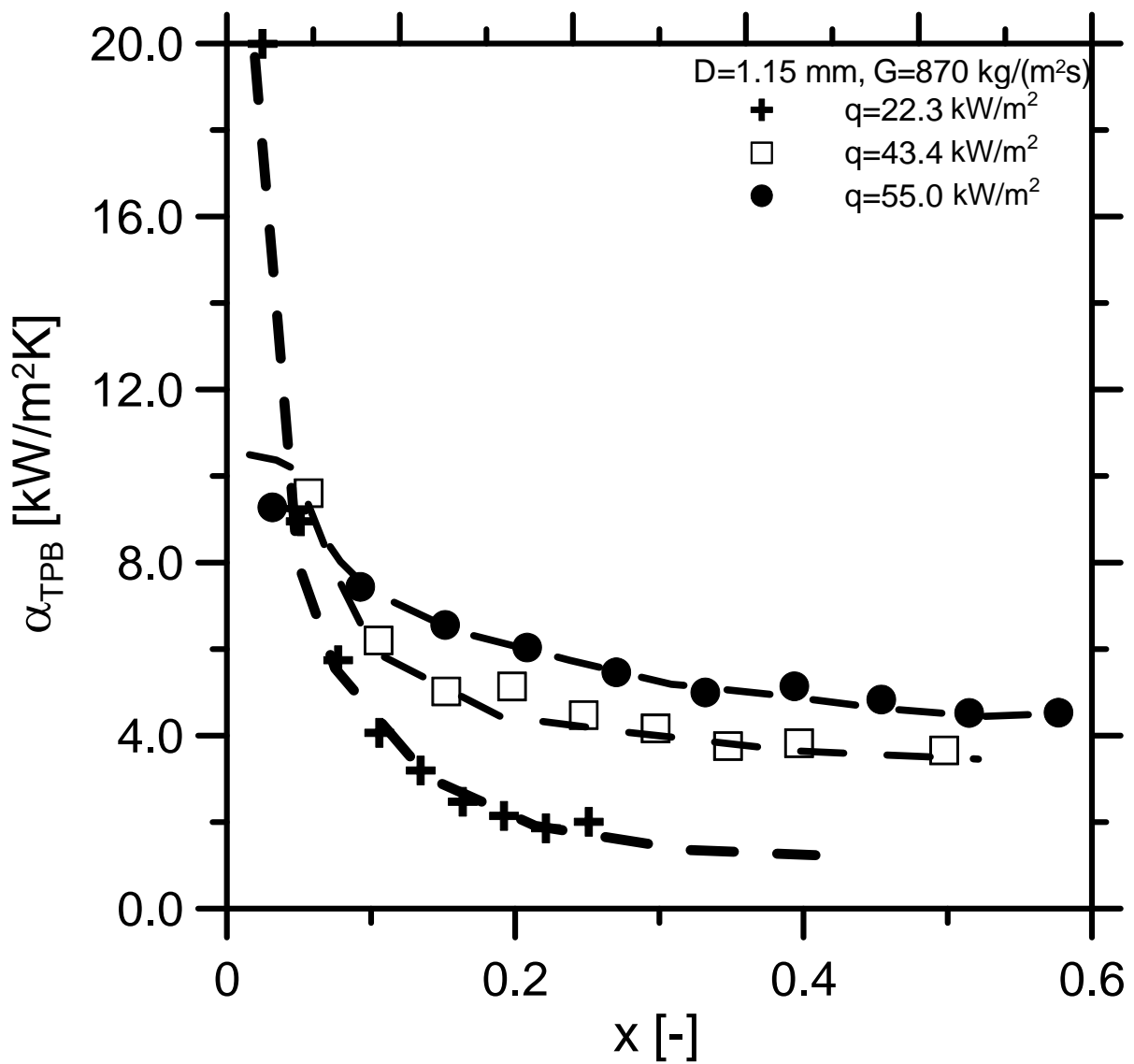


Figure 12. Distributions of heat transfer coefficient with respect to quality for fixed values of mass velocity and varying heat flux, $D=1.15 \text{ mm}, G=870 \text{ kg}/(\text{m}^2\text{s})$.

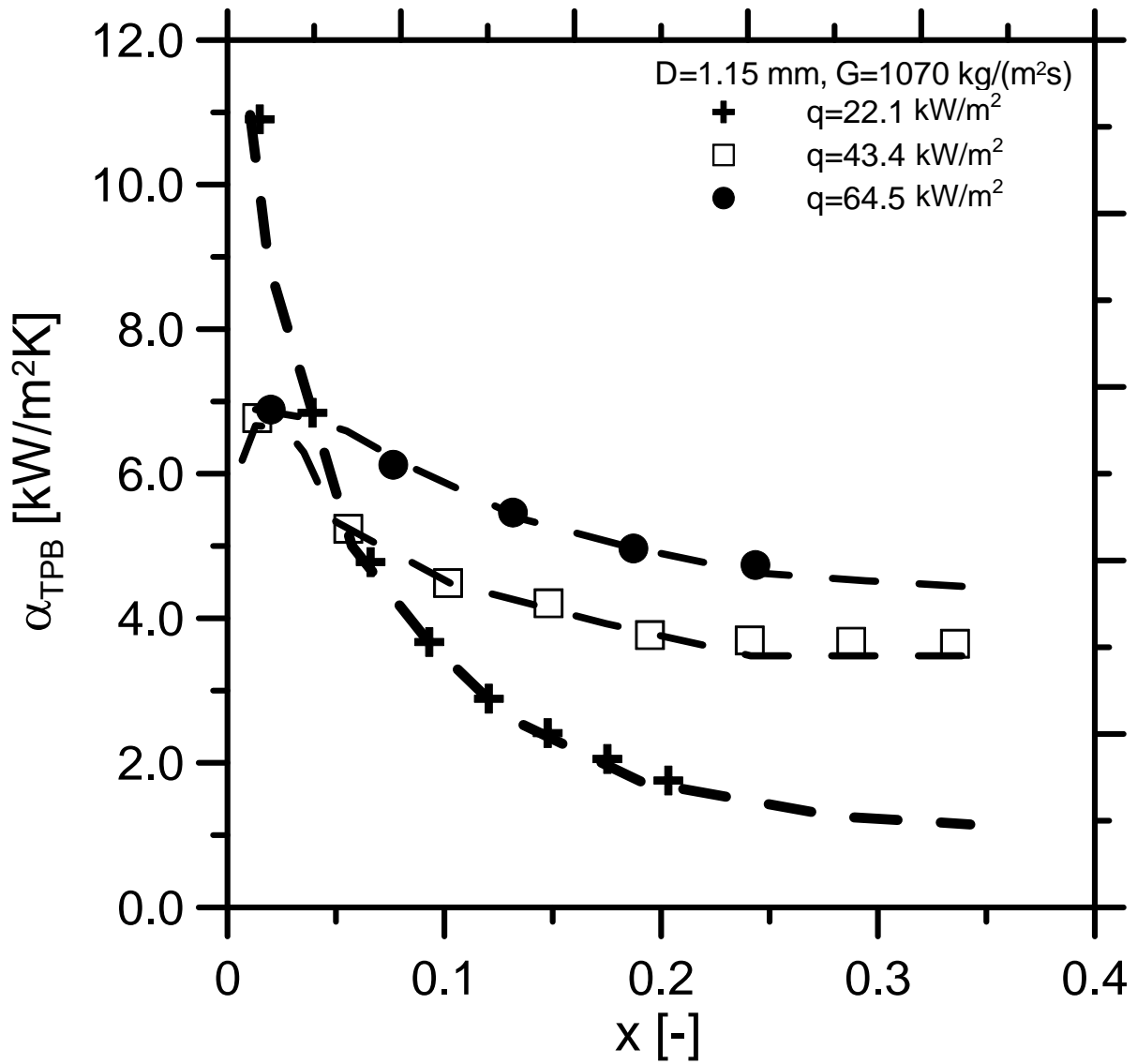


Figure 13. Distributions of heat transfer coefficient with respect to quality for fixed values of mass velocity and varying heat flux, $D=1.15 \text{ mm}$, $G=1070 \text{ kg/(m}^2\text{s)}$.

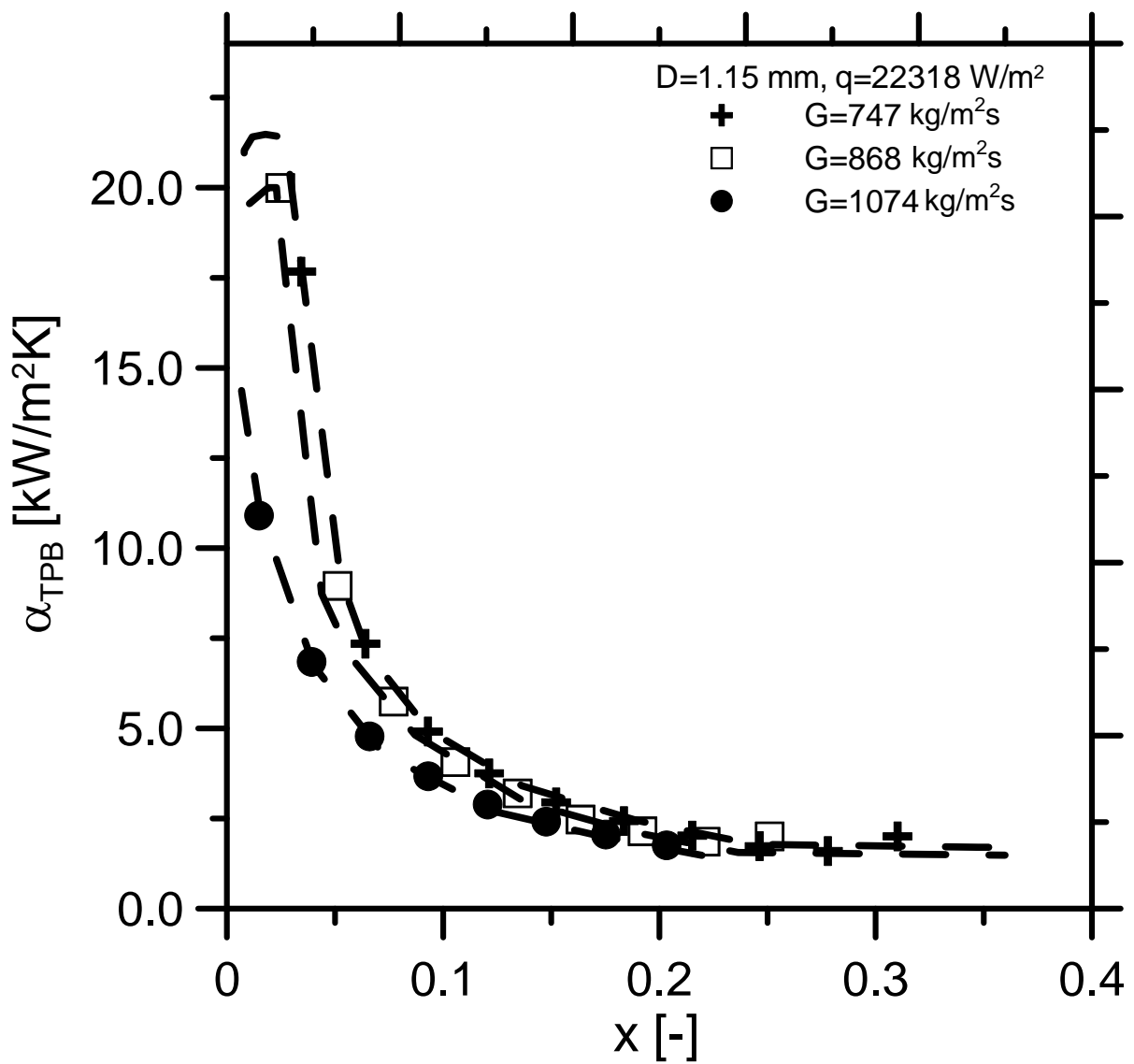


Figure 14. Distributions of heat transfer coefficient with respect to quality for fixed values of heat flux and varying mass velocity, $D=1.15 \text{ mm}, q=22318 \text{ W/m}^2$.

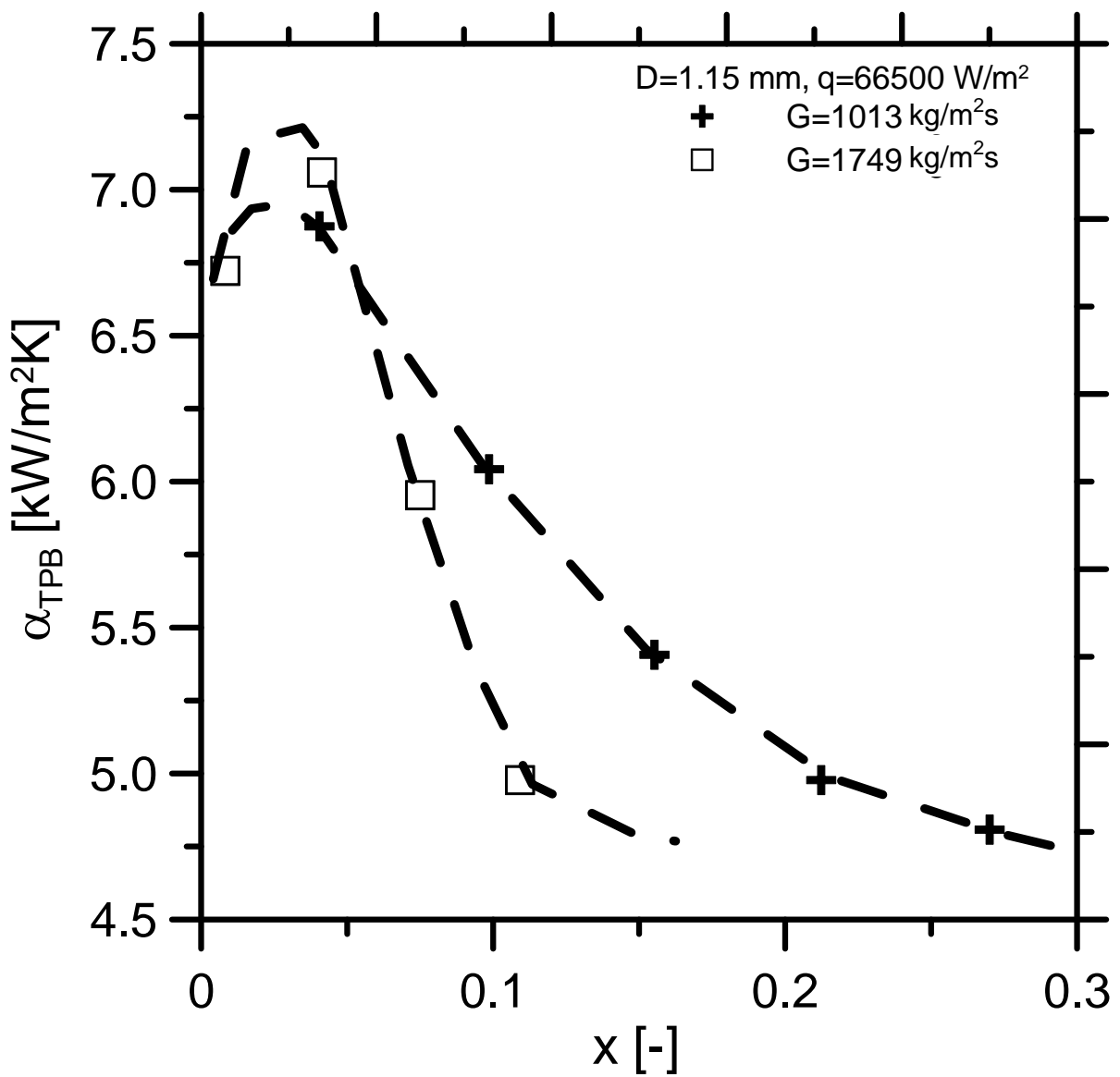


Figure 15. Distributions of heat transfer coefficient with respect to quality for fixed values of heat flux and varying mass velocity, $D=1.15 \text{ mm}, q=66500 \text{ W/m}^2$.

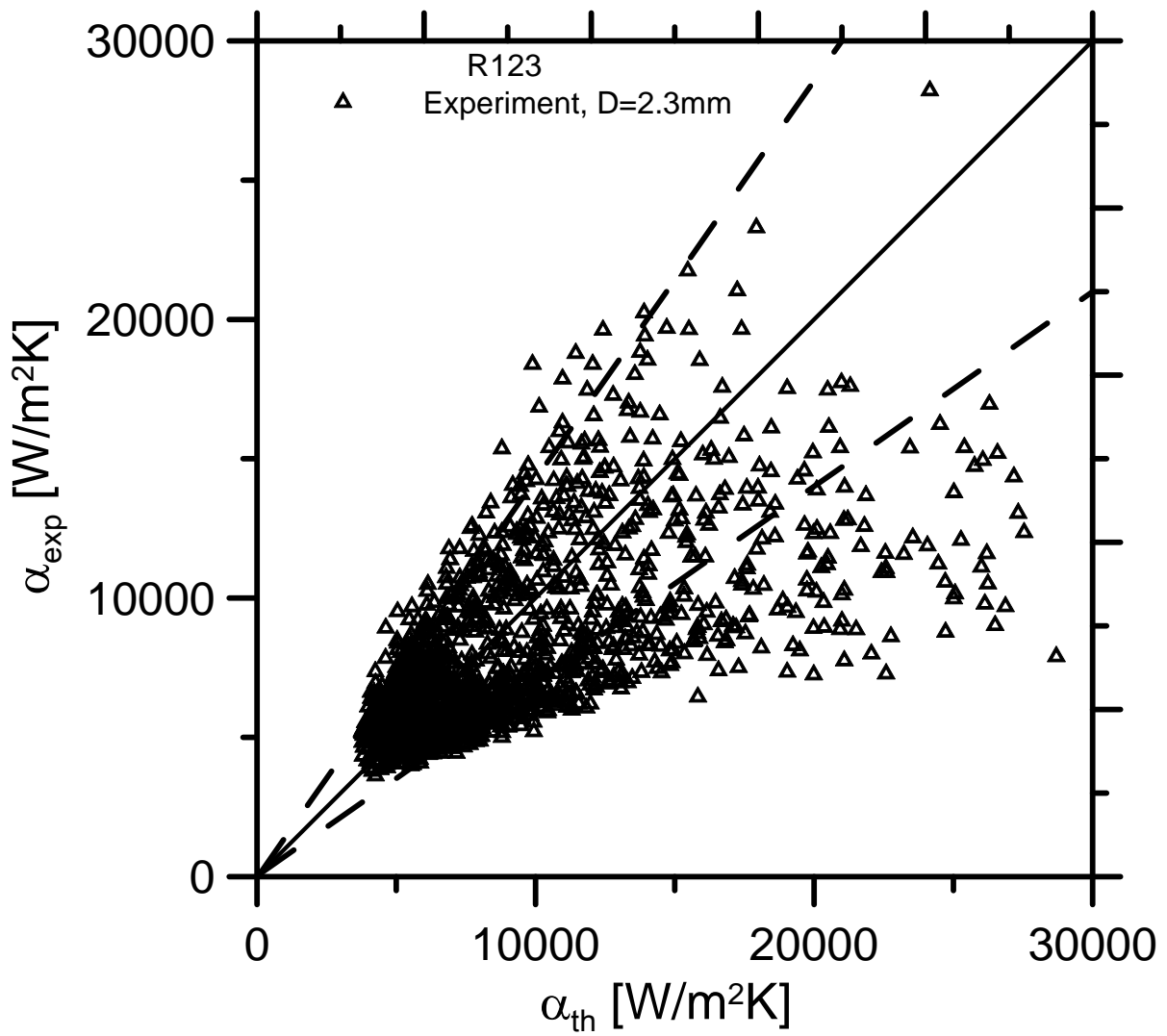


Figure 16. Experimental heat transfer coefficient as a function of heat transfer coefficient determined by expression (1), D=2.3 mm.

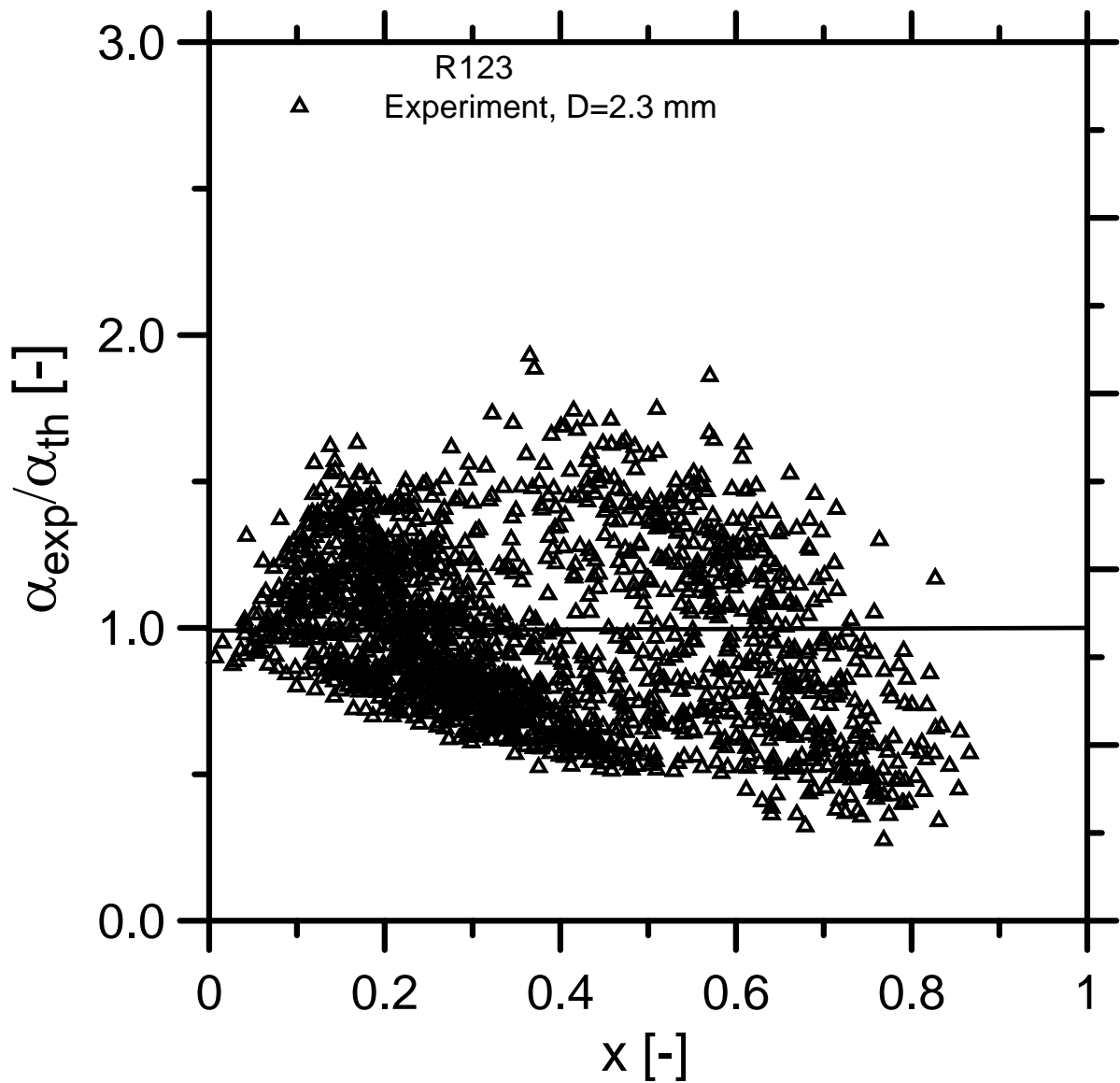


Figure 17. Ratio of experimental heat transfer coefficient to a value calculated by expression (1) as a function of quality, $D=2.3$ mm.

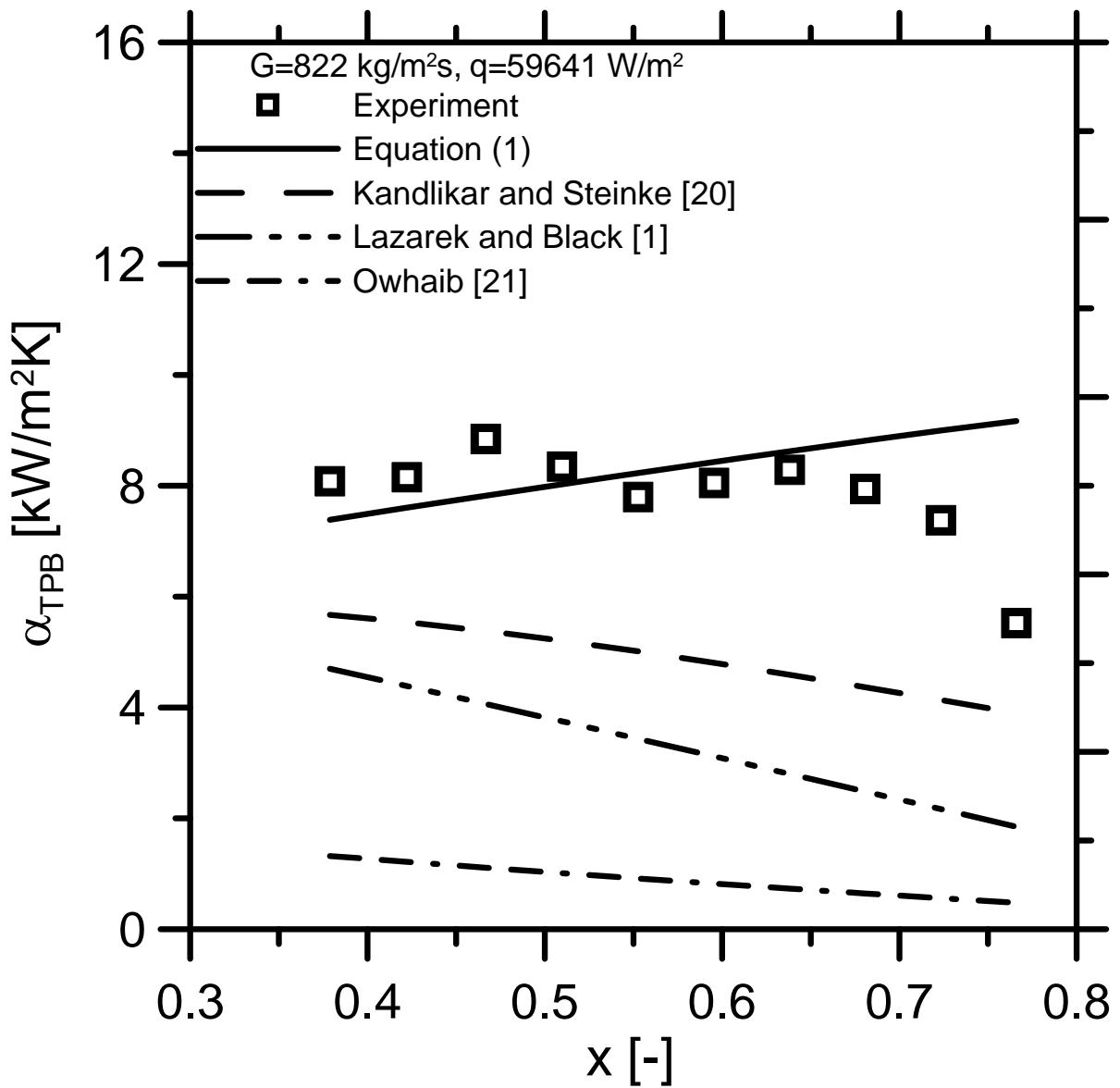


Figure 18. Comparison of obtained experimental data with other correlations for small diameter channel as a function of quality, $G=822 \text{ kg/m}^2\text{s}$, $q=59641 \text{ W/m}^2$, $d=2.3 \text{ mm}$.

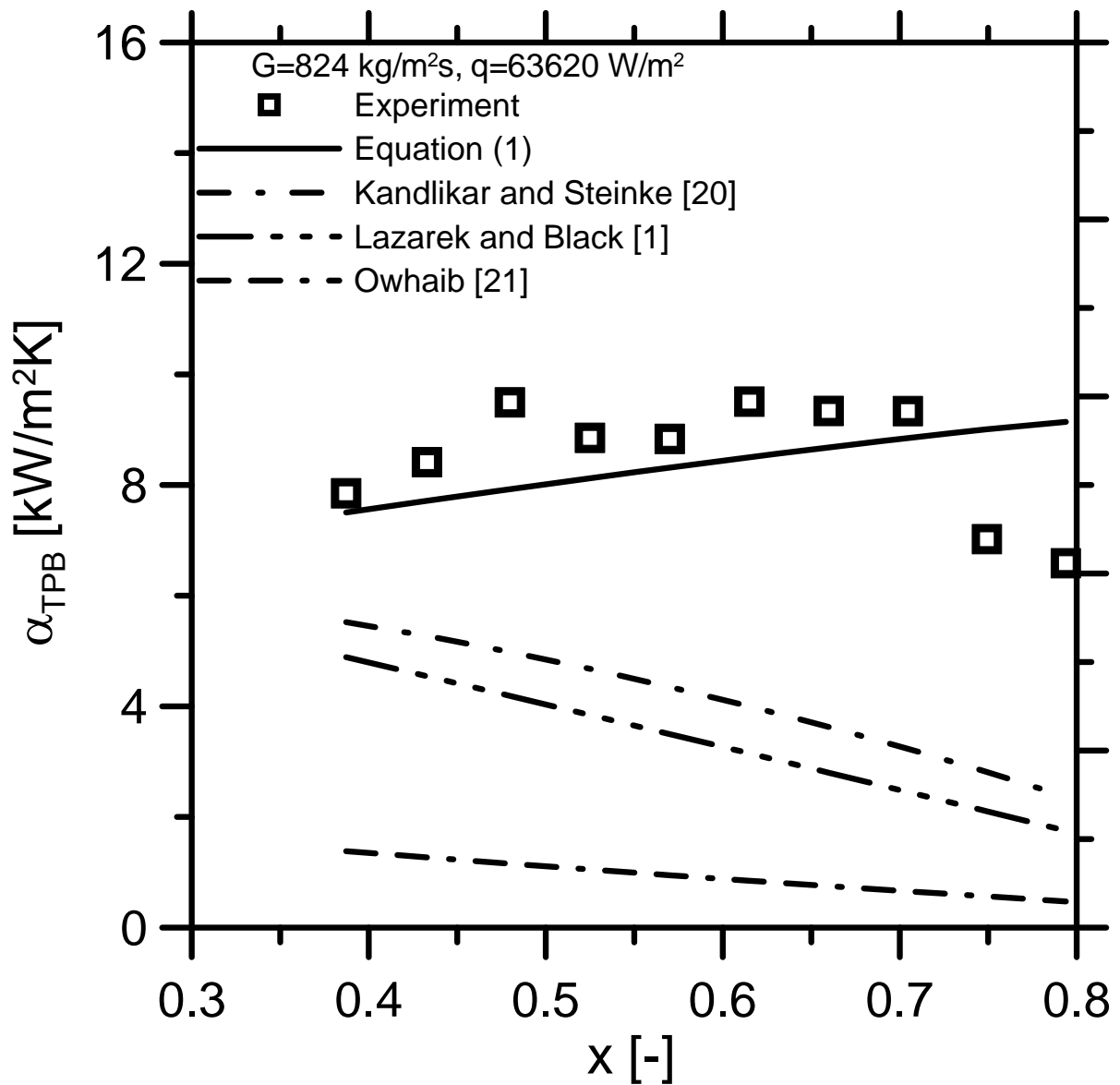


Figure 19. Comparison of obtained experimental data with other correlations for small diameter channel in function of quality, $G=824 \text{ kg/m}^2\text{s}$, $q=63620 \text{ W/m}^2$, $d=2.3 \text{ mm}$.

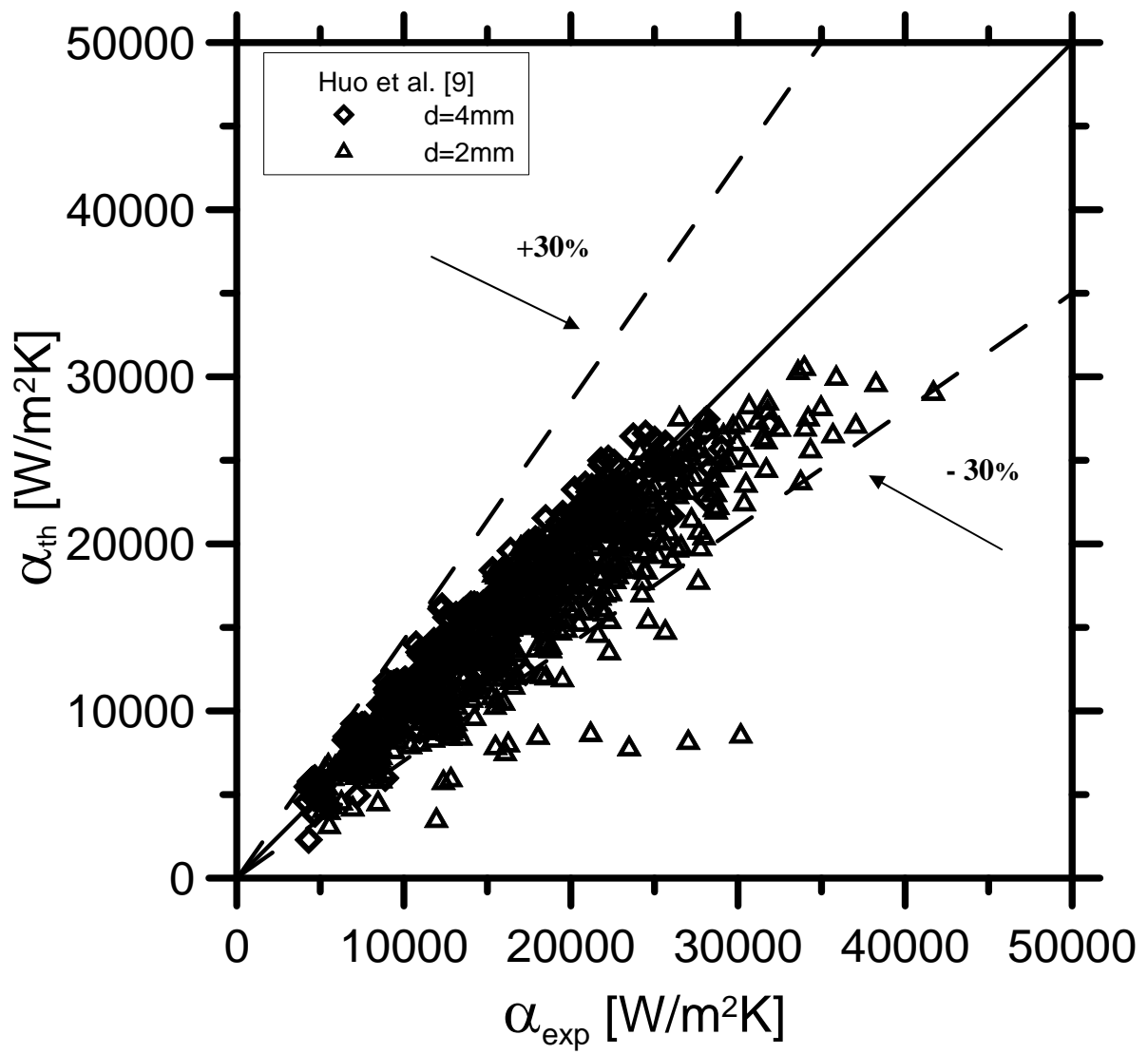


Fig. 20. Data due to Huo et al. [9] reduced with correlation (1).

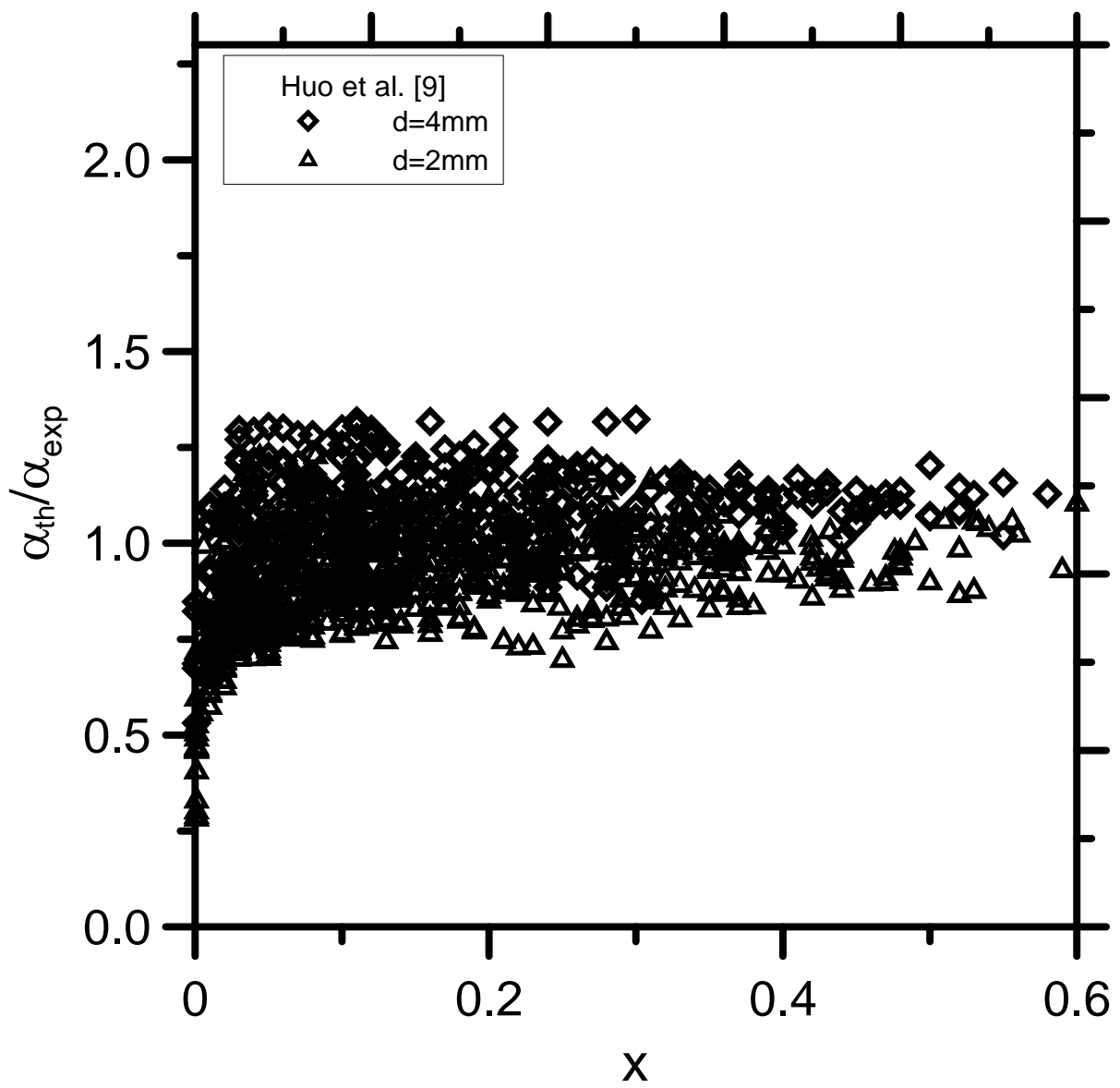


Fig. 21. Data due to Huo et al. [9] versus quality reduced with correlation (1).

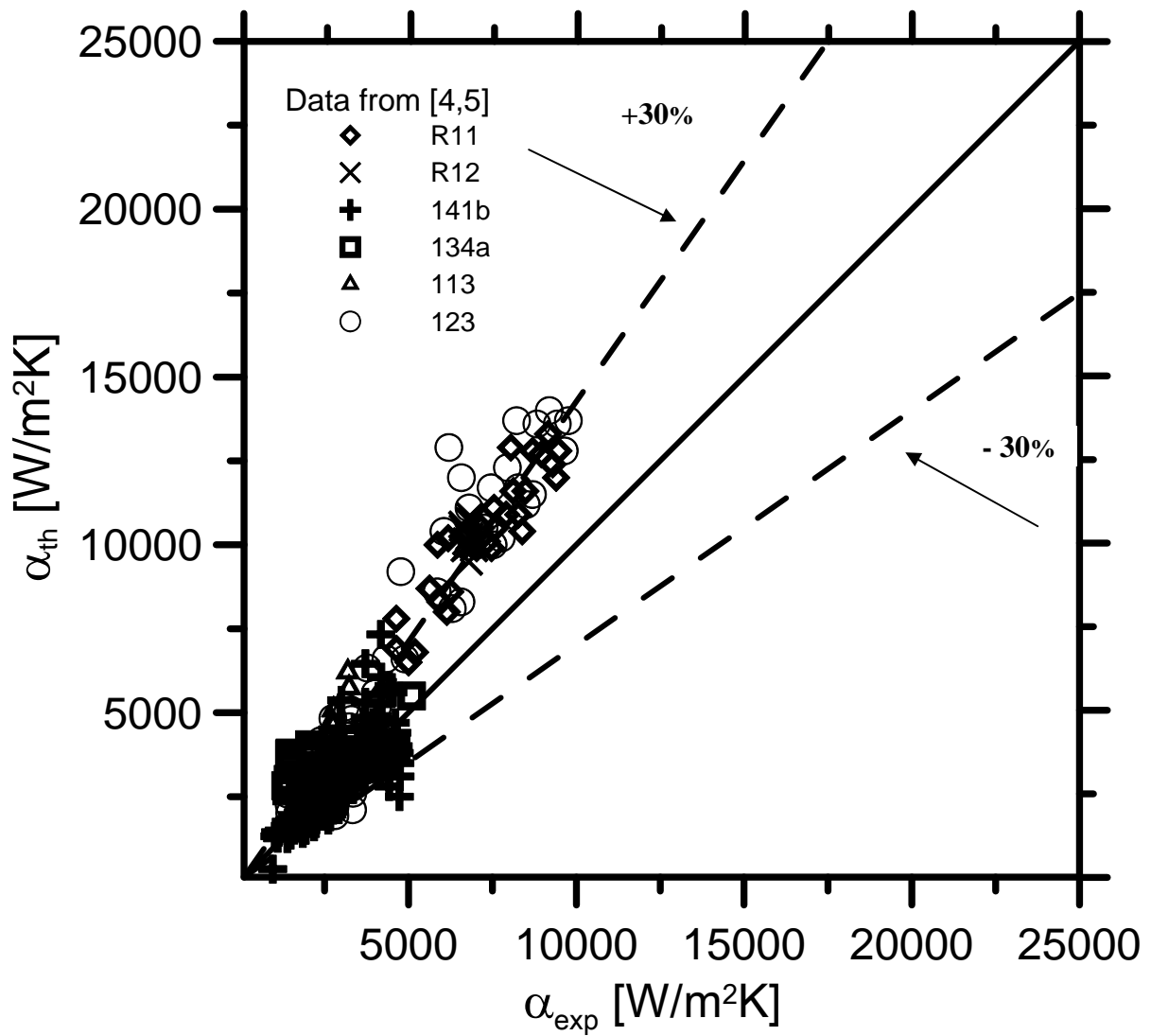


Fig. 22. Comparisons with experimental data due to Tran et al. [5] and Wambsganss et al. [4]

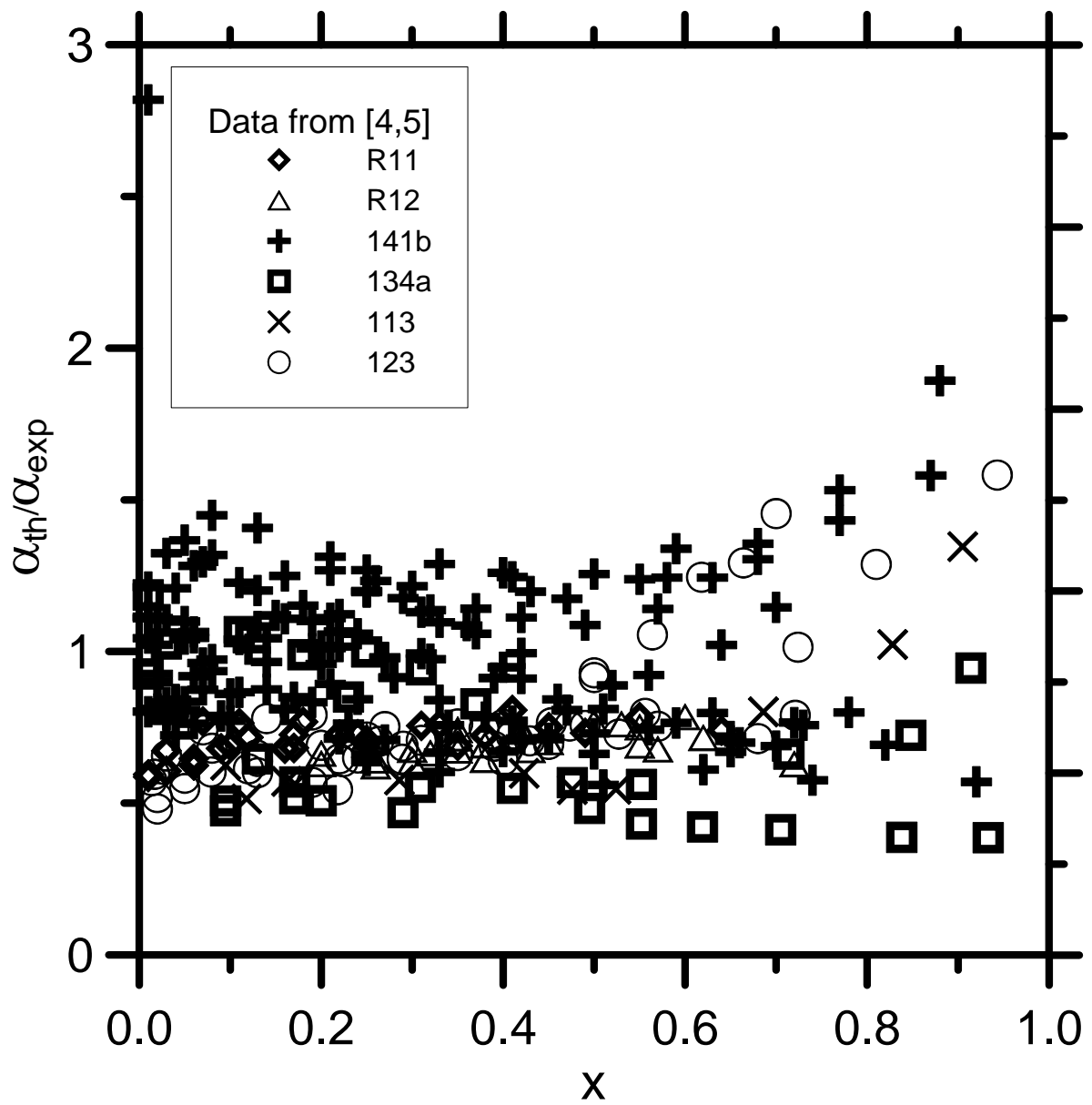


Fig. 23. Comparisons with experimental data due to Tran et al. [5] and Wambsganss et al. [4]

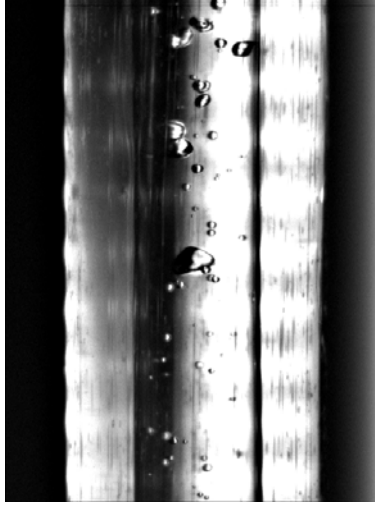


Figure 24. Beginning of nucleate boiling, $q = 39.7 \text{ kW/m}^2$, $G = 2883 \text{ kg/m}^2\text{s}$, $t_{\text{in}} = 22.51^\circ\text{C}$.

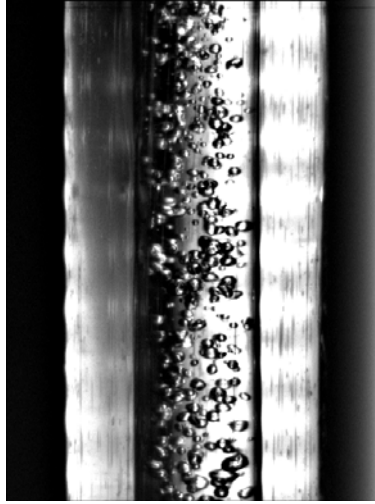


Figure 25. Developed nucleate boiling, $q = 39.7 \text{ kW/m}^2$, $G = 3650 \text{ kg/m}^2\text{s}$, $t_{\text{in}} = 30.75 \text{ }^\circ\text{C}$.

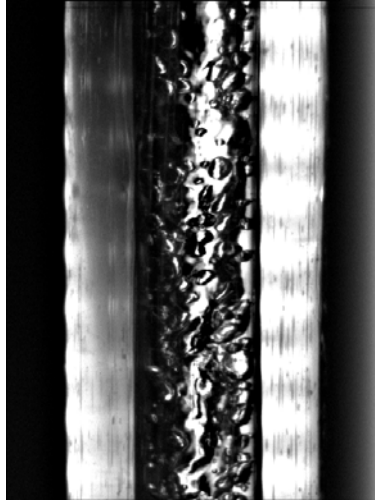


Figure 26. Wispy-annular flow boiling, $q = 39.7 \text{ kW/m}^2$, $G = 2237 \text{ kg/m}^2\text{s}$, $t_{\text{in}} = 41.53 \text{ }^\circ\text{C}$.

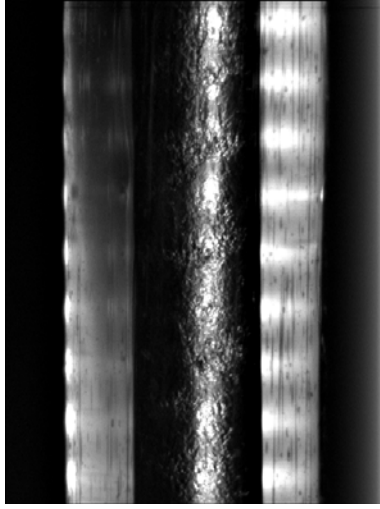


Figure 27. Mist-annular flow boiling, $q = 39.7 \text{ kW/m}^2$, $G = 783 \text{ kg/m}^2\text{s}$, $t_{\text{in}} = 54.09 \text{ }^\circ\text{C}$.



Dariusz Mikielwicz is a Professor employed by the Gdansk University of Technology, Gdansk, Poland since 1996. He received his MSc degree from the Gdansk University of Technology (1990), Ph.D. degree from the University of Manchester (1994) and in 2002 he presented his habilitation dissertation at the Gdansk University of Technology. In years 1994-1996 he worked as an engineer at the Berkeley Nuclear Laboratories, Nuclear Electric plc, Gloucestershire, UK. His research interest is in the field of modeling of two-phase flows both during boiling and condensation, efficient and precise jet and microjet cooling of hot surfaces, and recently renewable energy. He is currently working on enhanced heat transfer and condensation in heat exchangers, capillary effects in porous media and microjet technology.



Michal Klugmann is a lecturer at Gdansk University of Technology, Poland. He obtained his MSc and PhD from the Faculty of Mechanical Engineering of Gdansk University of Technology in 2004 and 2010 respectively. His research interests include heat exchange in mini and microchannels, microelectronics, energetics and alternative energy sources. His scientific activity is focused on experimental investigations. He is currently working on condensation during the two-phase flow in small diameter channels.



Jan Wajs is currently a lecturer at the Faculty of Mechanical Engineering of the Gdansk University of Technology, Poland. He received his MSc degree from Gdansk University of Technology in 2000. He presented his PhD dissertation in 2007 also to the Board of the Faculty of Mechanical Engineering of the GUT and was awarded the PhD degree. The area of his research activity include experimental investigations and mathematical modelling of heat transfer during flow boiling and condensation in the large scale and minichannels, designing of compact heat exchangers, heat recovery systems based on the Organic Rankine Cycle. Recently the thermal-hydraulics of nuclear power plant becomes his additional field of interest.